

**THE REPUBLIC OF TURKEY**  
**THE PRE-FEASIBILITY STUDY**  
**ON**  
**THE DIKILI-BERGAMA GEOTHERMAL DEVELOPMENT PROJECT**  
**FINAL REPORT**

**DECEMBER, 1987**

**JAPAN INTERNATIONAL COOPERATION AGENCY**

M	P	N
J		R
87-160		



**THE REPUBLIC OF TURKEY**

**THE PRE-FEASIBILITY STUDY**

**ON**

**THE DİKİLİ-BERGAMA GEOTHERMAL DEVELOPMENT PROJECT**

**FINAL REPORT**

JICA LIBRARY



1041711C13

**DECEMBER, 1987**

**JAPAN INTERNATIONAL COOPERATION AGENCY**

国際協力事業団		
受入 月日	88. 3. 22	314
登録No.	17325	64.3 MPN

## PREFACE

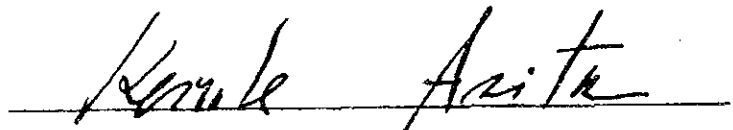
In response to the request of the Government of the Republic of Turkey, the Japanese Government decided to conduct a survey on the Dikili-Bergama Geothermal Development Project and entrusted the survey to the Japan International Cooperation Agency. The JICA sent to Turkey a survey team headed by Mr. Yasuhiko Ejima of West Japan Engineering Consultants Inc., three times from June, 1987 to November, 1987.

The team, with the cooperation of the officials concerned of the Government of Turkey, conducted a field survey on geology, geochemistry, geophysics and heat flow with a view to assessing geothermal potentiality in the Dikili-Bergama area. After the team returned to Japan, further studies were made and the present report has been prepared.

I hope that this report will serve for the geothermal development in Turkey and contribute to the promotion of friendly relations between our two countries.

I wish to express my deep appreciation to the officials concerned of the Government of the Republic of Turkey for their close cooperation extended to the team.

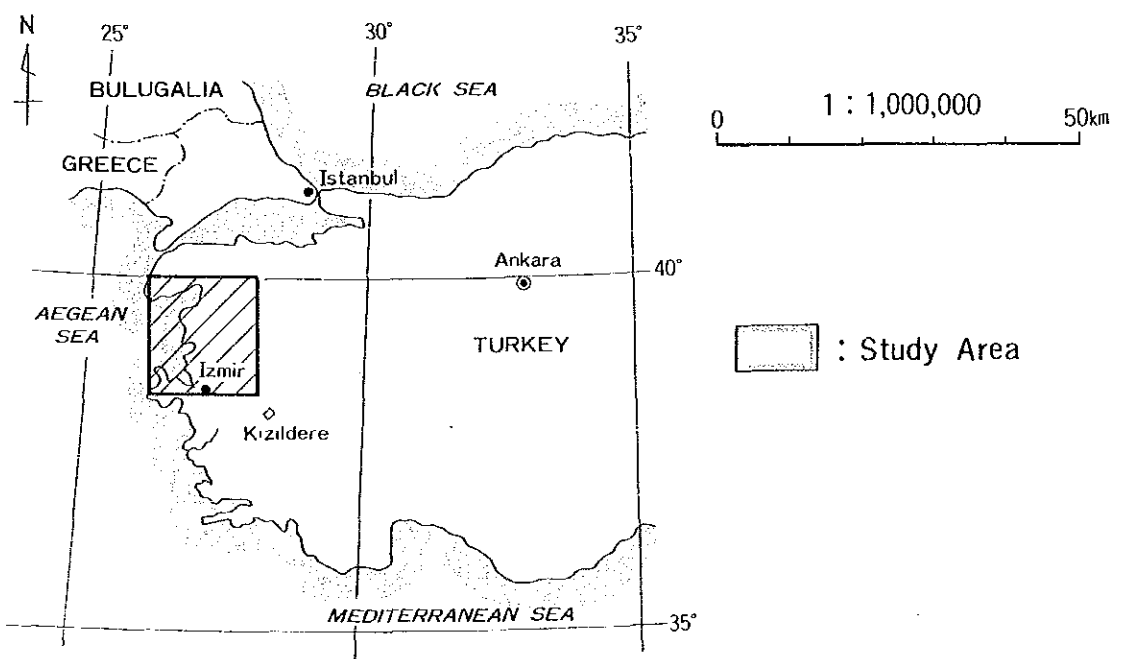
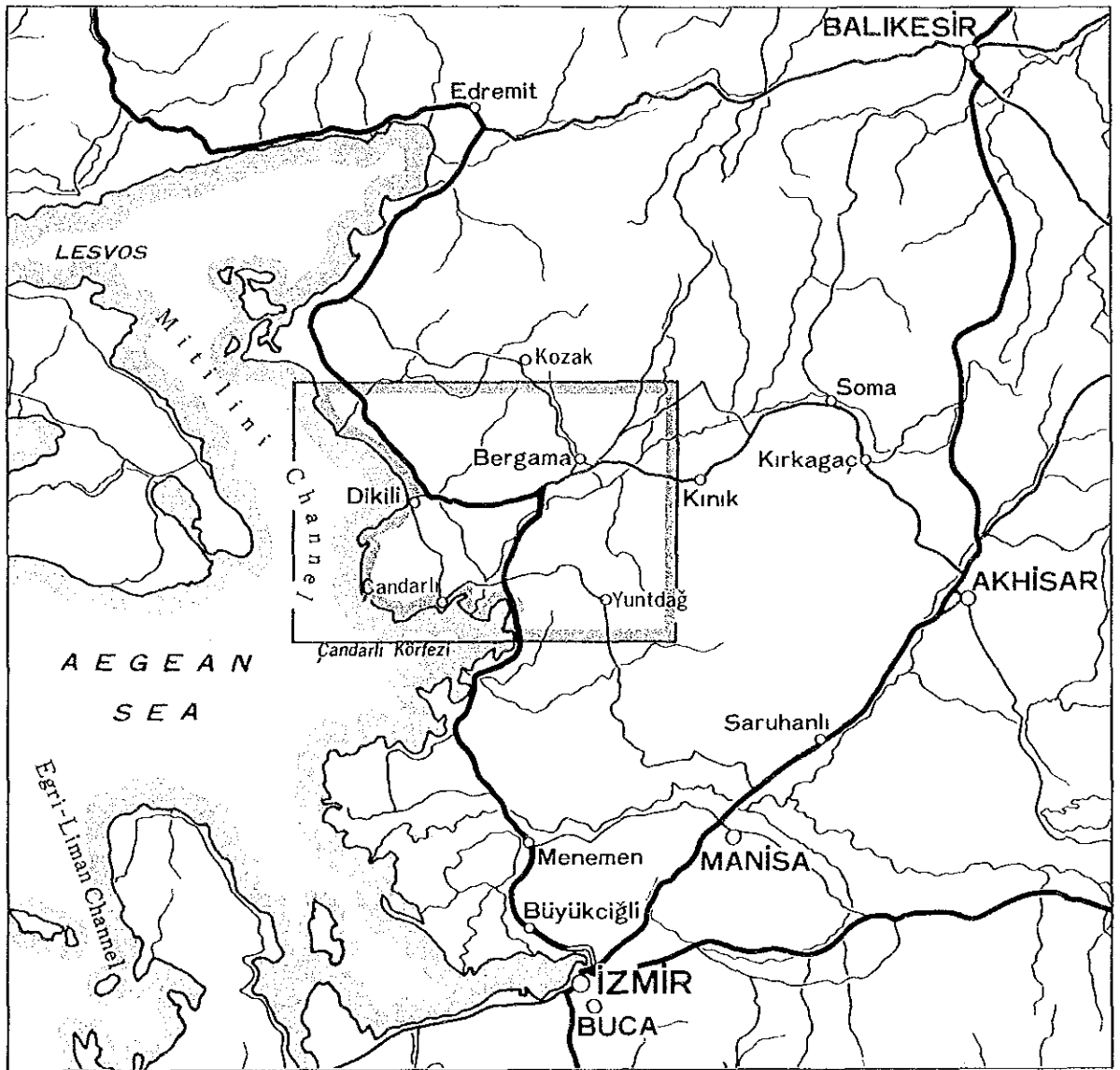
December, 1987

A handwritten signature in black ink, appearing to read 'Keisuke Arita', is written over a horizontal line.

Keisuke Arita  
President

Japan International Cooperation Agency

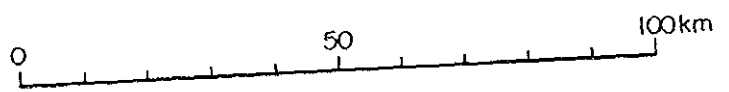
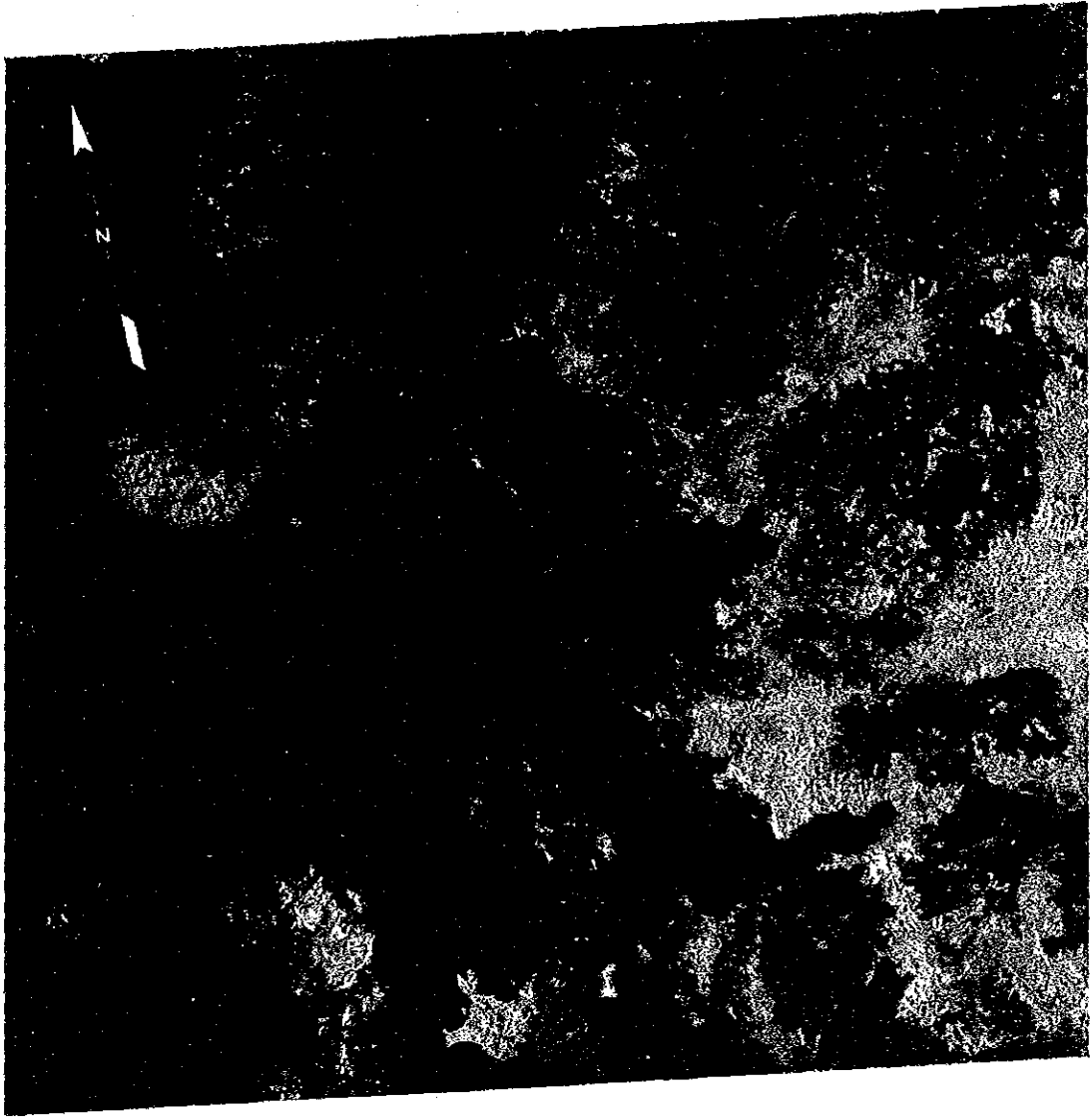




Location Map of Dikili-Bergama Geothermal Area

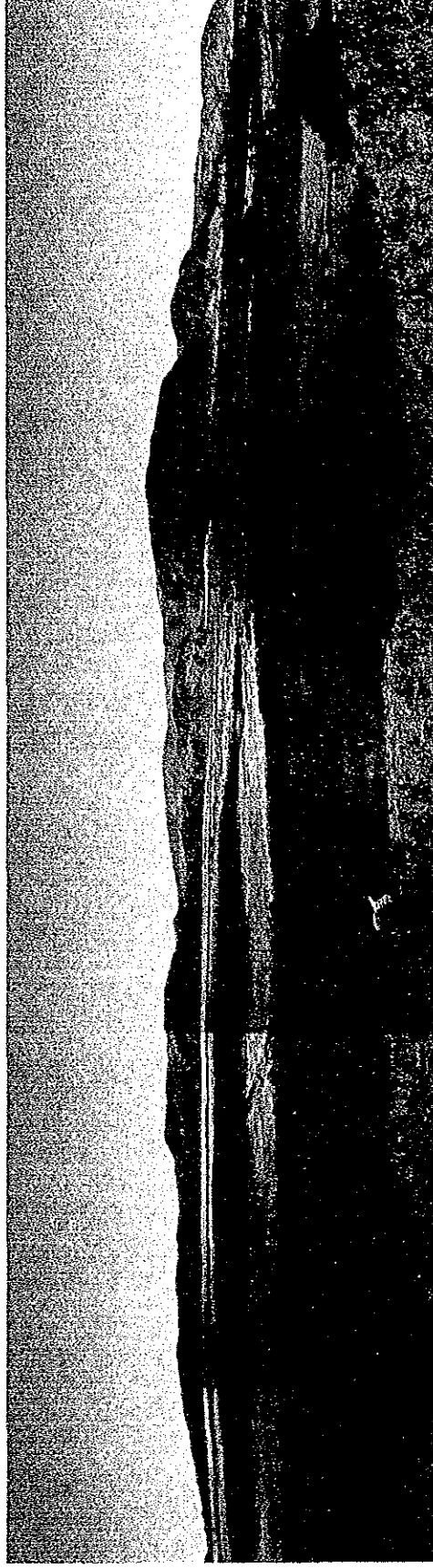






Color - Composite Landsat Image of Study Area  
(LANDSAT-5 18 MAY, 1984)





Panorama of the Kaynarca geothermal area



**THE PRE-FEASIBILITY STUDY  
ON  
THE DİKİLİ-BERGAMA GEOTHERMAL DEVELOPMENT PROJECT  
IN  
THE REPUBLIC OF TURKEY**

**(Final Report)**

**CONTENTS**

	Page
Preface	
Conclusion	
Recommendation	
Chapter I. Introduction	
I.1 Background of the study . . . . .	1
I.2 Objective of the study . . . . .	1
I.3 Procedure of the study . . . . .	2
I.4 Organization and staff of the study . . . . .	4
I.4.1 Organization . . . . .	4
I.4.2 Staff . . . . .	4
I.5 Progress of the study . . . . .	7
I.6 Outline of the survey area . . . . .	8
I.7 List of conducted surveys . . . . .	8
Chapter II. Results of the pre-feasibility study	
II.1 Outline of the first stage exploration . . . . .	13
II.1.1 Summary of survey results . . . . .	13
II.1.2 Regional geological structure and geothermal activity . . . . .	21
II.1.3 Conceptual model . . . . .	29
II.1.4 Selection of the prospective area for the second stage exploration . . . . .	30

	Page
II.2	Outline of the second stage exploration . . . . . 30
II.2.1	Summary of survey results . . . . . 30
II.2.2	Subsurface geological structure . . . . . 40
II.2.3	Volcanism and history of geothermal activity . . . . . 43
II.2.4	Chemical characteristics and temperature of reservoir fluid . . . . . 44
II.2.5	Conceptual model . . . . . 49
II.2.6	Selection of the prospective area for the third stage exploration . . . . . 50
II.3	Results of the third stage exploration . . . . . 50
II.3.1	Detailed geological mapping . . . . . 50
II.3.2	CSAMT survey . . . . . 81
II.3.3	Mise-à-la-masse survey . . . . . 125
II.3.4	Thermal gradient survey . . . . . 146

### Chapter III. Integrated assessment

III.1	Delimitation of the geothermal reservoir and modelling of the geothermal system . . . . . 214
III.1.1	Delimitation of the geothermal reservoir . . . . . 214
III.1.2	Conceptual geothermal model . . . . . 214
III.2	Assessment of the geothermal potential (feasibility of electric power development) . . . . . 219
III.2.1	Assessment of geothermal potential . . . . . 219
III.2.2	Feasibility of electric power development in the Kaynarca area . . . . . 220

### Chapter IV. Future development plan

IV.1	Plan of the future development . . . . . 221
IV.2	Multi-purpose utilization of the geothermal resource . . . . . 221
IV.3	Prediction of scale deposition in future geothermal utilization scheme and recommendation on scale prevention method . . . . . 222

	Page
IV.3.1 Prediction of scale deposition .....	222
IV.3.2 Scale prevention method .....	224
Appendix	

## LIST OF FIGURES AND TABLES

### (FIGURE)

- Fig. I.1.1 Flow chart of the geothermal study for the Dikili-Bergama area in Turkey
- Fig. II.1.1 Main tectonic block and radial diagrams for lineament of each geological block
- Fig. II.1.2 Geological interpretation map from Landsat image
- Fig. II.1.3 Distribution map of Pyroclastic rocks (Tp) and Youngest Yuntdağ volcanics (Tyu<sub>3</sub>)
- Fig. II.1.4 Geological interpretation map from aerial photographs
- Fig. II.1.5 Geological map in Dikili-Bergama geothermal area
- Fig. II.1.6 Location and measured temperature of hot springs in the Dikili-Bergama geothermal field
- Fig. II.1.7 Sampling sites of hot spring waters in the Dikili-Bergama geothermal field
- Fig. II.1.8 Piper tri-linear plots of hot springs in the Dikili-Bergama geothermal field
- Fig. II.1.9 Deuterium and oxygen-18 isotope ratios of hot spring and cold water (surface water) in the Dikili-Bergama geothermal field
- Fig. II.1.10 Reservoir temperature calculated by using silica thermometer in the Dikili-Bergama geothermal field
- Fig. II.1.11 Conceptual model of Dikili-Bergama geothermal area
- Fig. II.1.12 Survey area for second stage exploration
- Fig. II.2.1 Alteration zone map



- Fig. II.2.2 Fluid flow pattern of the Dikili-Kaynarca system
- Fig. II.2.3 Tectonic lines relating to geothermal activity
- Fig. II.2.4 Detailed bouguer anomaly map ( $\rho = 2.4$ )
- Fig. II.2.5 Detailed residual gravity map ( $\rho = 2.4$ )
- Fig. II.2.6 Geological map of Dikili-Ovacık area
- Fig. II.2.7 Geological cross section of Dikili-Ovacık area
- Fig. II.2.8 Hydrogeochemical model of the Dikili-Kaynarca system in the Dikili-Bergama geothermal field
- Fig. II.2.9 Smoothed iso-concentration contour map of Hg in soil gas
- Fig. II.2.10 Smoothed iso-concentration contour map of Hg in soil
- Fig. II.3.1 Bird's-eye view of the Kaynarca geothermal area
- Fig. II.3.2 Geological map of the Kaynarca geothermal area
- Fig. II.3.3 Geological cross sections of Kaynarca geothermal area
- Fig. II.3.4 Distribution of faults around Kaynarca
- Fig. II.3.5 Fracture pattern of Yuntdağ volcanics I in the Kaynarca geothermal area
- Fig. II.3.6 Fracture pattern of Demirtas pyroclastic rocks in the Kaynarca geothermal area
- Fig. II.3.7 Fracture pattern of Yuntdağ volcanics III in the Kaynarca geothermal area
- Fig. II.3.8 Composite map showing fracture pattern in the Kaynarca geothermal area
- Fig. II.3.9 Pattern of hydrothermal veins in the Kaynarca geothermal area

- Fig. II.3.10 Plot of width and orientation of hydrothermal veins in the Kaynarca geothermal area
- Fig. II.3.11 Fracture pattern in each formation
- Fig. II.3.12 Presumed stress field in the Kaynarca geothermal area
- Fig. II.3.13 Geothermal structure of the Kaynarca geothermal area
- Fig. II.3.14 Survey configuration for CSAMT measurement
- Fig. II.3.15 Flow of analysis for CSAMT measurement
- Fig. II.3.16 Apparent resistivity map (128 Hz)
- Fig. II.3.17 Apparent resistivity map (4 Hz)
- Fig. II.3.18 Apparent resistivity map (0.25 Hz)
- Fig. II.3.19 Apparent resistivity pseudosection and 1D inversion results (A line)
- Fig. II.3.20 Apparent resistivity pseudosection and 1D inversion results (B line)
- Fig. II.3.21 Apparent resistivity pseudosection and 1D inversion results (C line)
- Fig. II.3.22 Apparent resistivity pseudosection and 1D inversion results (D line)
- Fig. II.3.23 Apparent resistivity pseudosection and 1D inversion results (E line)
- Fig. II.3.24 Apparent resistivity pseudosection and 1D inversion results (F line)
- Fig. II.3.25 Apparent resistivity pseudosection and 1D inversion results (G line)

- Fig. II.3.26 Apparent resistivity pseudosection and 1D inversion results (H line)
- Fig. II.3.27 Apparent resistivity pseudosection and 1D inversion results (I line)
- Fig. II.3.28 Apparent resistivity pseudosection and 1D inversion results (J line)
- Fig. II.3.29 Apparent resistivity pseudosection and 1D inversion results (K line)
- Fig. II.3.30 Apparent resistivity pseudosection and 1D inversion results (L line)
- Fig. II.3.31 Apparent resistivity pseudosection and 1D inversion results (M line)
- Fig. II.3.32 Apparent resistivity pseudosection and 1D inversion results (N line)
- Fig. II.3.33 Apparent resistivity pseudosection and 1D inversion results (O line)
- Fig. II. 3.34 Apparent resistivity pseudosection and 1D inversion results (P line)
- Fig. II.3.35 Apparent resistivity pseudosection and 1D inversion results (Q line)
- Fig. II.3.36 Apparent resistivity pseudosection and 1D inversion results (R line)
- Fig. II.3.37 Apparent resistivity pseudosection and 1D inversion results (S line)
- Fig. II.3.38 Apparent resistivity pseudosection and 1D inversion results (T line)
- Fig. II.3.39 Apparent resistivity pseudosection and 1D inversion results (U line)

- Fig. II.3.40 Longitudinal conductance map
- Fig. II.3.41 Elevation map of top of the electrical basement
- Fig. II.3.42 Resistivity map of the electrical basement
- Fig. II.3.43 Apparent resistivity pseudosections (I–P line)
- Fig. II.3.44 2-D resistivity structure model of M line
- Fig. II.3.45 Comparison of pseudosections along M line (observed and modeling result)
- Fig. II.3.46 Geothermal structure estimated from CSAMT
- Fig. II.3.47 Equipment layout for Mise-à-la-masse measurement
- Fig. II.3.48 Flow of analysis for Mise-à-la-masse measurement
- Fig. II.3.49 V/I map (point source)
- Fig. II.3.50 V/I map (200 m casing pipe)
- Fig. II.3.51 Lineament estimated from V/I distribution
- Fig. II.3.52 V/I map (500 m casing pipe)
- Fig. II.3.53 Theoretical potential map
- Fig. II.3.54 Apparent resistivity map (point source)
- Fig. II.3.55 Apparent resistivity map (200 m casing pipe)
- Fig. II.3.56 Apparent resistivity map (500 m casing pipe)
- Fig. II.3.57 Residual potential map (point source)
- Fig. II.3.58 Residual potential map (200 m casing pipe)
- Fig. II.3.59 Residual potential map (500 m casing pipe)

- Fig. II.3.60 Difference of low potential anomalies in the case of different current source
- Fig. II.3.61 Fault trending NW-SE direction estimated from low potential anomaly shape in northeastern part of survey area
- Fig. II.3.62 Geothermal structure estimated from electrical surveys
- Fig. II.3.63 Location of thermal gradient holes
- Fig. II.3.64 Geologic column
- Fig. II.3.65 Heat flow of thermal gradient hole
- Fig. II.3.66 Distribution of alteration in thermal gradient hole
- Fig. II.3.67 Distribution of declination of field rock sample
- Fig. II.3.68 Stereonet plot of dip and strike of fracture in DG-1
- Fig. II.3.69 Homogenization temperature of fluid inclusion in DG-1
- Fig. II.3.70 Comparative diagram of rock properties against depth
- Fig. II.3.71 Chemical composition of rock in thermal gradient hole
- Fig. II.3.72 Chemical composition of core and cuttings plotted onto the AFM diagram
- Fig. II.3.73 Chemical composition of core and cuttings plotted onto the AL-(Ca+Na+K)-Mg diagram
- Fig. II.3.74 Deuterium and oxygen-18 isotope ratios of hot spring and cold water (surface water) in the Dikili-Bergama geothermal field
- Fig. II.3.75 Relationship between Cl concentration and delta-D value of geothermal matter in the Dikili-Bergama geothermal field
- Fig. II.3.76 Relationship between Cl and HBO<sub>2</sub> concentration

- Fig. II.3.77 Silica temperature by mixing model
- Fig. II.3.78 Simplified model on geothermal fluid estimated by using chemical analysis data of temperature gradient holes
- Fig. II.3.79 Geological cross section of the Kaynarca geothermal area
- Fig. II.3.80 Isothermal line of the Kaynarca geothermal area
- Fig. III.1.1 Synthetic interpretation map
- Fig. III.1.2 Conceptual model of the Kaynarca geothermal area
- Fig. IV.3.1 An example of carbonate scale deposited in a production well (Otake geothermal field)
- Fig. IV.3.2 Injection system of chemicals for carbonate scale prevention

**(TABLE)**

- Table II.1.1 Geological succession of Dikili-Bergama geothermal area
- Table II.3.1 Geological succession of the Kaynarca geothermal area
- Table II.3.2 Results of temperature recovery test
- Table II.3.3 Results of heat flow calculation
- Table II.3.4 Stratigraphy of thermal gradient holes
- Table II.3.5 Petrography of rock-forming minerals
- Table II.3.6 Result of x-ray analysis
- Table II.3.7 Result of measurement of fractures in core (DG-1)
- Table II.3.8 Fluid inclusion data
- Table II.3.9 Results of rock property measurement

Table II.3.10 Chemical composition of core and cuttings

Table II.3.11 Chemical composition of hot water from thermal gradient hole

Table II.3.12 Geochemical temperature and C1/B and C1/As atomic ratios  
in the waters sampled from DG-1, DG-2, DG-3 and others





## CONCLUSION

The Study was conducted in three stages in the Dikili-Bergama geothermal area in the Republic of Turkey to select the most prospective area and to evaluate the geothermal resource potential.

### I. Summary of the results of the study

There are twenty or more hot springs in the survey area. However, hot springs of higher than 60°C are distributed around Yuntdağ volcanic III in the southwest of the survey area, and are located along faults in the Dikili-Bergama graben. The results of the Study are useful to make a conceptual model of the Kaynarca geothermal area. The most prospective geothermal area in Dikili-Bergama geothermal area is summarized as follows.

1. It is considered that the heat source of the geothermal activity in the Kaynarca area is related to post volcanism of the Sulu Kaya lava and the Koca Tepe lava, which were interpreted as the latest volcanism in Dikili-Bergama geothermal area. Geothermal activity in the Kaynarca area is, however, judged to be the retrogressive period, because the latest volcanism was inferred to be in more than two million years ago in the Pliocene age and on a small scale.
2. The origin of geothermal fluid in the Kaynarca geothermal area is considered to be meteoric water permeated to ground at northeast of Kaynarca, and its circulating time is calculated to be longer than 75 years by Tritium data. Therefore, the geothermal system of Kaynarca is considered to be a hydrothermal convection system and is similar to other active geothermal areas in the world.
3. The chemical characteristics of hot water discharging at Kaynarca indicate that geothermal fluid of 180 to 200°C is reserved in a fracture zone in Tertiary volcanic rocks, Yuntdağ I at depth. An isotope thermometer, however, suggests temperature higher than 220°C at depth.
4. The extent of the geothermal reservoir is delimited as about 1 km<sup>2</sup> south of Kaynarca from the results of the Study, such as Hg anomaly by the geochemical survey, extent of high longitudinal conductance zone by CSAMT survey and low residual potential zone by Mise-à-la-masse survey. Deep geothermal fluid is supposed to be flowing up through the intersection of NE-SW trending fault and NW-SE trending fault.
5. According to the thermal gradient survey, there are no significant reservoirs down to 700 m to the north of Kaynarca. A deep geothermal reservoir is

thought to exist deeper than 800 m, because a prospective reservoir is usually formed in the electrical basement and the thickness of the low resistivity zone of Kaynarca is 600 to 800 m around the supposed fault zones.

6. The problems of calcium carbonate scale deposition in production wells (which will cause a high cost for steam development) and high concentration of noncondensable gas (which will decrease the efficiency of power generation) will make it difficult to develop a geothermal power plant in the future.

As mentioned above, it is scarcely expected that geothermal reservoir of higher than 200°C is formed shallower than 1,000 m in the Kaynarca area. In conclusion, the activity (geothermal potential) of the Kaynarca area seems to be low in comparison with other active geothermal areas in the world, even with those of the Kizildere and Germencik geothermal areas in Turkey.

## **II. Feasibility of power plant development in the Kaynarca area**

The characteristics of the geothermal reservoir in the Kaynarca area (such as temperature, depth, extent together with high concentration of noncondensable gas) will make it difficult to develop a geothermal power plant from economical point of view.

## **III. Technical transfer**

The JICA team carried out the Study in accordance with a flow chart of exploration (which was formulated by considering the characteristics of the project area), and in close cooperation with Turkish counterparts. Through the Study, the JICA Team transferred geothermal exploration technologies to their Turkish counterparts, such as purpose, analyzing method and interpreting method of each survey, in addition to operating system and maintenance method of equipment donated by JICA. The Turkish counterparts now understand fully the methods and technologies needed to carry out geothermal development by themselves in other areas in Turkey.

The Study contributed to the improvement geothermal exploration techniques in Turkey, and will then effectively promote geothermal development in Turkey.

## **RECOMMENDATION**

The Kaynarca area, which was selected as the most promising area in the Dikili-Bergama geothermal area, was evaluated as not feasible economically at this moment to develop as a sole purpose of power generation.

The evaluation, however, does not mean to deny the possibility to develop the geothermal resource for multi purpose utilization. Therefore from the viewpoints of multi utilization of the geothermal resource, it is necessary to carry out further explorations to confirm the geothermal potential at depth for the purpose to study the possibility in detail.



## CHAPTER I. INTRODUCTION



## CHAPTER I. INTRODUCTION

### I.1 Background of the study

The Republic of Turkey (hereinafter referred to as "Turkey") has conducted geothermal resource development by General Directorate of Mineral Research and Exploration (MTA) for diversification and domestic supply of energy since 1960. Subsequent investigations pointed out the great potential of geothermal resource in Turkey. The first geothermal field leading to utilization for power generation was explored in Kızıldere-Denizli in 1968. The Kızıldere power plant, the first geothermal power plant in Turkey, was constructed in 1984, is now operating with a generation capacity of 20 MW.

The development of geothermal resources in Turkey will contribute to solve the energy shortage of the country. But the limited number of rigs for drilling geothermal wells together with the high costs of geothermal exploration slows down these projects.

With this background, the Government of Turkey requested the government of Japan to implement the pre-feasibility study on the geothermal development project in accordance with the relevant laws and regulations in force in Japan.

In response to the request by the government of Turkey, Japan International Cooperation Agency (JICA) carried out the preparatory study for the geothermal project in Turkey in July, 1985, and proposed "Dikili-Bergama" area as a promising site.

The JICA preliminary study team visited Turkey again in January 1986, and the scope of work with regard to the Pre-Feasibility Study on Dikili-Bergama Geothermal Development Project (hereinafter referred to as "the Study") was signed.

Based on the scope of work, JICA decided to send a pre-feasibility study team to Turkey headed by Mr. Ejima on 24 June, 1986.

### I.2 Objective of the study

The objective of the Study is to assess the potential of geothermal resource in the Dikili-Bergama geothermal area, by means of geoscientific methods, including geological survey, geochemical survey, geophysical exploration and thermal gradient survey. Finally a further development plan of the project area is considered.

### I.3 Procedure of the study

The Study proceeded step by step in accordance with the flow chart of the Study (Fig. I.1.1) which was formulated to select the most prospective area in the Dikili-Bergama area (1,000 km<sup>2</sup>) in west Anatoria, to select the site for the thermal gradient survey holes, to evaluate the potential of the most prospective area, and finally to prepare a further development plan. Outlines of each stage exploration are as follows:

#### 1. The first stage exploration

During the first stage exploration, the Inception Report was made by reviewing the existing data, and then geological structure interpretation, geological reconnaissance and a preliminary geochemical survey were conducted. As a result of the first stage exploration, a prospective area (274 km<sup>2</sup>), in which four hot springs of Kaynarca, Dikili, Kocaoba and Mentese are located, was selected for the second stage exploration. A concrete plan for the second stage exploration was formulated on the basis of the first stage exploration.

Regional geological data, orogenic movement data, plate tectonics data magmatic activity data and seismic activity data of the country were collected and were analyzed to review of existing data. Geochemical data were analyzed to study the hydrothermal system of the region and mechanism of the geothermal system of the prospective area.

#### 2. The second stage exploration

Measurements of physical property of rocks, hydrothermal alteration survey, geochemical and hydrological survey, and gravity survey were conducted during the second stage exploration to select the most prospective area, and then a concrete plan of exploration for the most prospective area was formulated.

Geochemical and hydrological data were combined with the geological conceptual model to estimate the structure of the geothermal reservoir, the origin and flow of geothermal fluid, and then the temperatures of geothermal reservoir. A soil gas survey, namely CO<sub>2</sub>, Hg and Rn concentrations in soil gas, was conducted to clarify the structure of the prospective area. Regarding the gravity survey, the JICA team made the survey plan and conducted the supervision of data interpretation, and the Turkish counterpart conducted the field survey and data processing.



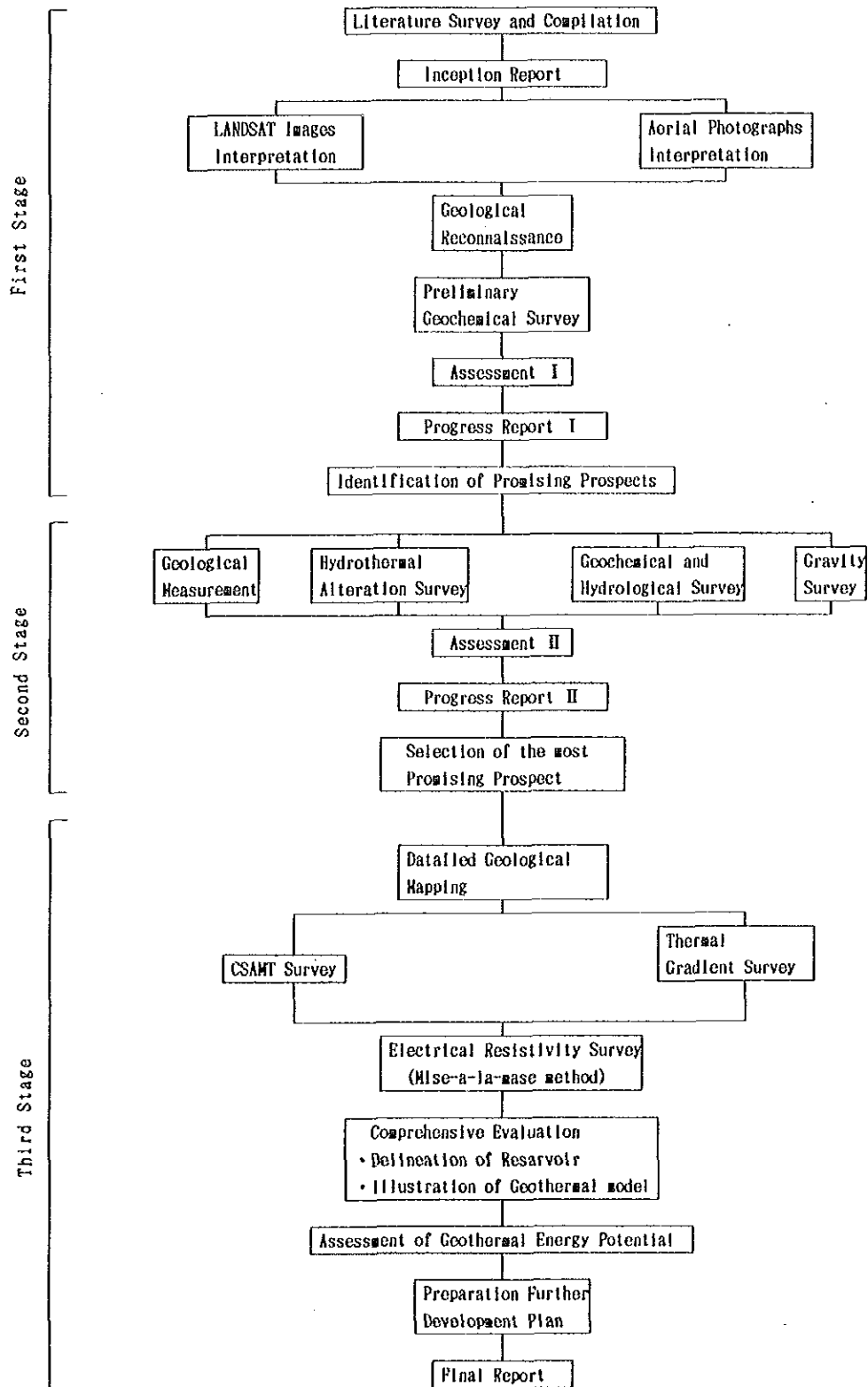


Fig I .1.1 Flow chart of the geothermal study for the Dikili-Bergama area in Turkey

The most prospective area (42 km<sup>2</sup>) for the third stage exploration was selected by the integrated analysis of all available data and also by understanding the problems of scale deposition.

### 3. The third stage exploration

Detailed geological survey, CSAMT survey, mise-à-la-masse and thermal gradient survey were conducted during the third stage exploration, and these data were utilized to delimit the reservoir within the most prospective area, and then to prepare a geothermal model. On the basis of all available data and on the comparison with other promising geothermal areas in the world, the potential of geothermal resource in the project area was evaluated, and a further development plan of the project area was recommended.

The study proceeded smoothly and on schedule. Each survey at each stage was conducted in close cooperation with the Turkish counterparts; furthermore technical transfer was performed during the Study.

## I.4 Organization and staff of the study

### I.4.1 Organization

In accordance with the Scope of Work, the following organizations were in charge of the Study.

#### Japan

Japan International Cooperation Agency  
(JICA)

West Japan Engineering Consultants,  
Inc. (JICA Team)

#### Turkey

General Directorate of Mineral Research  
and Exploration (M.T.A.)

Geothermal Division  
Energy Department  
M.T.A.

Izmir Regional Center  
M.T.A.

### I.4.2 Staff

The JICA Team and M.T.A. Team were organized into the following staff to carry out the Study.

### JICA Team

Project Manager	Yasuhiko EJIMA
Chief Geologist	Toshio FUJINO
Geologist	Hiroshi TAKAGI
Geologist	Naoto TAGUCHI
Chief Geochemist	Kanichi SHIMADA
Geochemist	Tatsuo IWANAGA
Chief Geophysicist	Tadahiko SHIMOIKE
Geophysicist	Koichi TAGOMORI
Geophysicist	Yoshihiro YONEDA
Geophysicist	Koichi MATSUO
Geophysicist	Yutaka MURAKAMI

### MTA Team

Project Manager (Assoc. Prof.)	Şakir ŞİMŞEK
Deputy Manager	Ali KOÇAK

### Geological Survey Unit

Geologist (Camp Chief)	Servet YILMAZER
Geologist	Ali İhsan GEVREK
Geologist	Tuncer EŞDER
Geologist	Zühal SÜNGER
Geologist	Ramazan PEKATAN

### Geochemical Survey Unit

Geochemist	Nazım YILDIRIM
Geochemist	Ziya SARIDAL
Geochemist	Işıl KAYRAN
Geochemist (Lab. Work)	Gülay ATAMAN
Geochemist (Lab. Work)	Süheyla TUNCER
Geochemist (Lab. Work)	Muzaffer ŞÖNMEZ

### CSAMT Survey, Mise-à-la-masse Survey, Logging Unit

Geophysicist (Chief)	Altan İÇERLER
Geophysicist (Camp Chief)	Tuğrul TOKGÖZ
Geophysicist (Camp Chief)	M. Emin ÖZGÜLER

Geophysicist	Kenan TEZCAN
Geophysicist	Kadircan AKTAŞ
Geophysicist	Mete YÜCEL
Logging Engineer	Mesut ÖNDER
Logging Engineer	İskender TUNCAY
Surveyor	Ümit KILIÇASLAN
Surveyor	Mehmet GÖKGÜL
Surveyor	Hüseyin ACAR

#### Gravity Survey Unit

Geophysicist	Serter GÖÇTÜ
Geophysicist	Arslan ÇINAR
Surveyor	Haydar KONAKÇI
Surveyor	Murat ÇETİNDAĞ

#### Drilling Unit

Drilling Engineer (Chief)	Abdullah GÜLGÖR
Drilling Engineer	Ali CANPOLAT
Drilling Engineer	Dmre BABÜR
Drilling Engineer	Mustafa BAŞIKARA

The JICA Team and the MTA Team thank to the following high ranking officials for their supports to realize the study.

General Manager	M. Sıtkı SANCAR
Deputy Manager	Askın VOLKAN
Head of Energy Dept. (Assoc. Prof.)	Güner ÜNALAN
Coordinator of Energy Dept.	Vedat YÜKSEL
Head of Geophysical Survey Dept.	Ferit ERDEN
Coordinator of Geophysical Survey Dept.	Tuncer ÜNAY
Coordinator of Geophysical Survey Dept.	Günay YALDIZ
Head of Drilling Dept.	Necdet AKBAŞLI
Head of Planning Dept.	Teoman ÖZGÜVEN
Coordinator of Planning Dept.	Engin ÇUBUKÇU
District Manager (Aegean)	Özer ÖLÇER

### I.5 Progress of the study

The study was implemented in three stages in accordance with the Scope of Work.

Stage	Survey Items	1986		1987	
		6	12	6	12
FIRST	LANDSAT image interpretation	7/21 5/24  8/2			
	Aerial photographs interpretation				
	Geological reconnaissance				
	Preliminary geochemical survey	8/22			
	Tentative report	8/13			
SECOND	Hydrothermal alteration survey	8/25  10/4			
	Geological measurement				
	Geochemical and hydrological survey	11/14			
	Gravity survey	8/25  9/22  12/8			
	Tentative report	12/10  2/22			
THIRD	Detailed geological map	1/6  3/15		2/15  3/15	
	CSAMT survey			5/25  7/24	
	Mise-a'-la-masse			5/25  8/8	
	Thermal gradient survey			5/25  7/18  8/2	
	Tentative report			10/30  11/30 10/1  11/13	
	Tentative Report	7/19  10/2  11/12		2/13  3/24  7/16  8/6	
	Progress Report I	8/23			
	Progress Report II			1/8	
	Draft Final Report			11/8	
	Final Report			12/10	

## 1.6 Outline of the survey area

The survey area is located between Bergama and Dikili, about 75 km north of İzmir, west Anatoria, Republic of Turkey. The Turkish counterparts prepared a project base camp in Dikili. It can be reached by plane and bus as follows:

Ankara	—————	İzmir	—————	Dikili
	(1)		(2)	
(1)	Domestic flight		50 minutes	
(2)	Bus		1 hour	

The main part of the survey area is composed of an alluvial plain formed by the Bakir river, and hills and highland in the north and south. The alluvial plain, hills and the highlands are formed by geologic tectonic movement, and the alluvial plain along the Bakir river is called the Dikili graben. Within the Dikili graben, the E-W extending plain is split into two at the mid point, one is in a northwest direction and reaches Dikili and the other is in a southwest direction and reaches Candarli. These geological conditions are considered to be closely related to the geothermal activity.

Geothermal manifestations such as hot springs, hot pools, calcareous sinter and hydrothermal alteration are distributed in the Dikili-Bergama graben, and there are no fumaroles. There are, however, also no fumaroles in the Kizildere and Germensik geothermal area, where the first geothermal power plant in Turkey is constructed and geothermal explorations have been continued. There are two remarkable hot springs, namely the Kaynarca and Dikili Ilicasi, around Dikili, however, comparatively less manifestations around Bergama. Several hot springs of 50 to 60 m diameter and 2 m depth are distributed in Kaynarca.

## 1.7 List of conducted surveys

The following surveys were conducted during the Study.

Stage		Contents
FIRST	<u>Geological survey</u>	
	LANDSAT image interpretation	80,000 km <sup>2</sup>
	Aerial photograph interpretation	1,500 km <sup>2</sup>
	Geological reconnaissance	2,200 km <sup>2</sup>
	<u>Preliminary geochemical survey</u>	
	Chemical analysis of hot spring	18 samples
	Isotopic analysis of hot spring	10 samples
	Isotopic analysis of surface water	18 samples
	Soil analysis	30 samples
	Gas analysis	30 samples
SECOND	<u>Geological survey</u>	
	Geological survey	274 km <sup>2</sup>
	Geological measurement	
	Microscopic observation	24 samples
	X-ray analysis	24 samples
	Physical property of rock	24 samples
	Age determination	10 samples
	Hydrothermal alteration survey	
	X-ray analysis	59 samples
	Chemical analysis of rock	20 samples
	<u>Geological and hydrological survey</u>	
	Chemical analysis of hot spring	26 samples
Isotopic analysis of hot spring	24 samples	
Isotopic analysis of surface water	26 samples	

Stage		Contents
	Soil gas (Hg, CO <sub>2</sub> , Rn) Soil (Hg) Temperature at one meter depth <u>Gravity survey</u> Survey area Number of stations	302 samples 302 samples 300 points  81 km <sup>2</sup> 693 stations
THIRD	<u>Geological survey</u> Detailed geological mapping  <u>Thermal gradient survey</u> Thermal gradient calculation  Geological measurement Microscopic observation X-ray analysis Fluid inclusion geothermometry Fracture analysis in core Physical property of rock Chemical analysis of rock Geochemical analysis Chemical analysis of discharging water  <u>CSAMT survey</u> Number of frequencies  Number of stations  <u>Mise-à-la-masse survey</u> Depth of current electrode  Number of stations	42 km <sup>2</sup>  683 m X 1 hole 200 m X 2 holes  21 samples 65 samples 7 samples 7 samples 11 samples 65 samples 3 samples  16  376 stations  0 m 200 m 500 m  188 stations



## CHAPTER II. RESULTS OF THE PRE-FEASIBILITY STUDY



## CHAPTER II. RESULTS OF THE PRE-FEASIBILITY STUDY

### II.1 Outline of the first stage exploration

#### II.1.1 Summary of survey results

The first stage exploration, literature survey and compilation, geological reconnaissance and preliminary geochemical survey were carried out by the JICA team.

##### 1. Literature survey and compilation

In the Dikili-Bergama geothermal area, geological, geochemical, geophysical and thermal gradient surveys had been conducted by MTA prior to the study.

Since the volcanic activity and tectonic movements are very intense in the Dikili-Bergama area, it is assumed that the heat source of the geothermal activity is caused by tectonism and volcanism. The reservoirs are expected in fracture zones and permeable zones in the sandstone, siltstone, conglomerate and limestone, belonging to pre-Tertiary basement. The Soma formation which is widely distributed probably act as a cap rock. The reservoir temperature estimated from geochemical thermometry (Na-K-Ca method) is 173°C.

##### 2. Geological structure interpretation

###### (1) Landsat images interpretation

Using Landsat data of 4 scenes (path-row; 180-21, 180-33, 181-32, 181-33), Landsat images were interpreted in Japan and on site, then field survey was carried out.

The western Anatoria provides four distinct tectonic lines and NE-SW trending lineaments in Fig. II.1.1. Of these lineaments, the main trend of N30°E is observed in Fig. II.1.2. In the Dikili-Bergama geothermal area, parallel lineaments through Bergama is distinct and extensive. The NE-SW trending lineaments partly form small grabens.

There are two kinds of fault and lineament; NE-SW and NW-SE trending. Along the NE-SW trending fault, felsic volcanism erupted phroclastic rocks in Fig. II.1.3. On the other hand, dome-shaped volcanoes were formed along NW-SE trending faults.

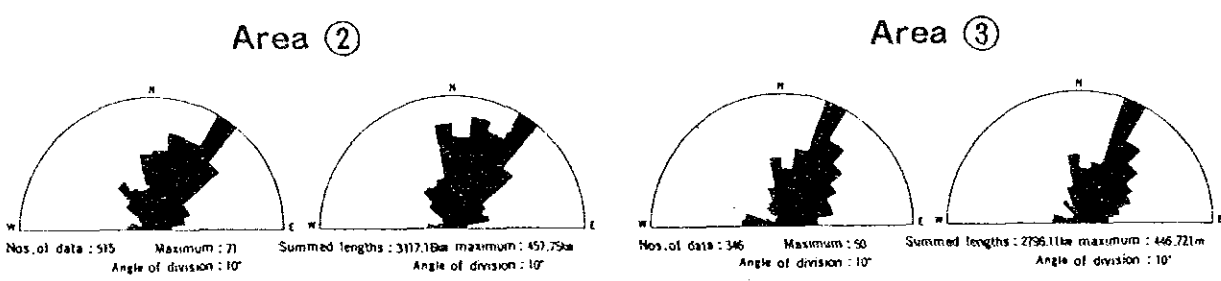
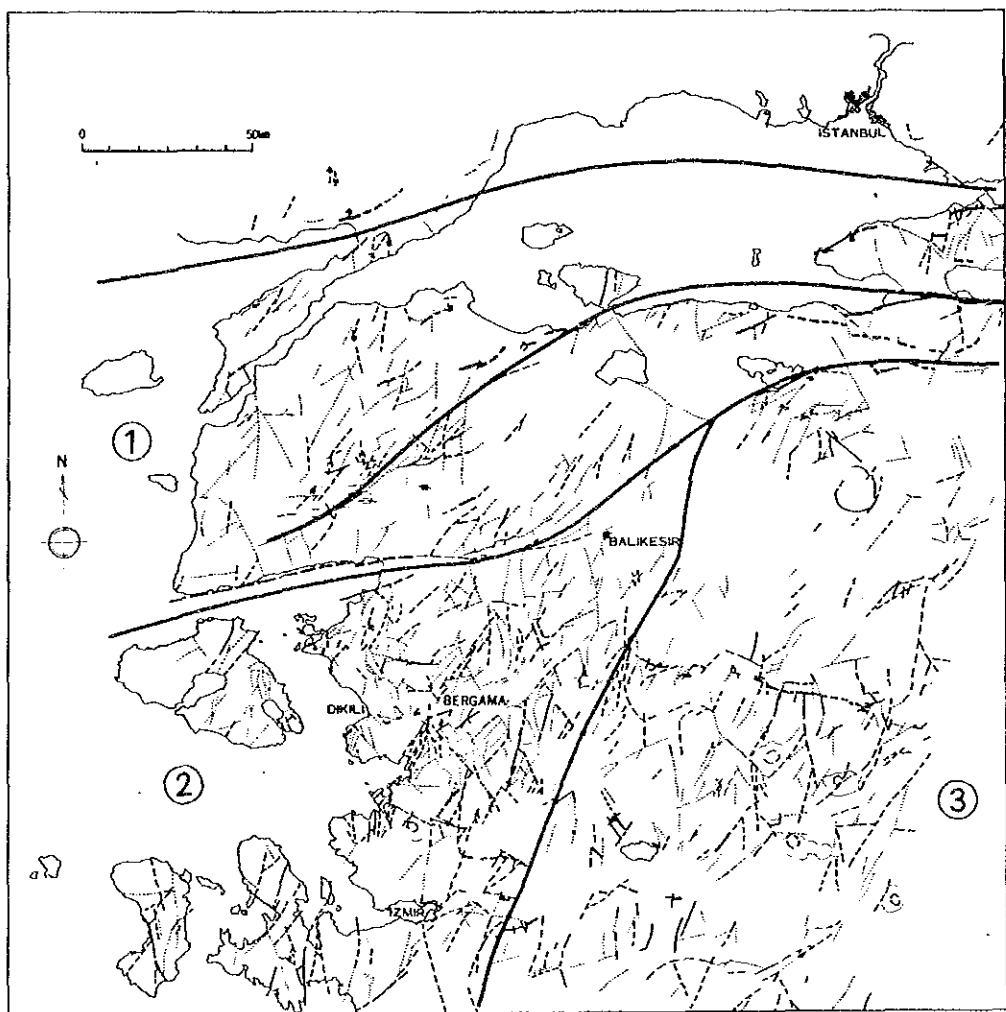
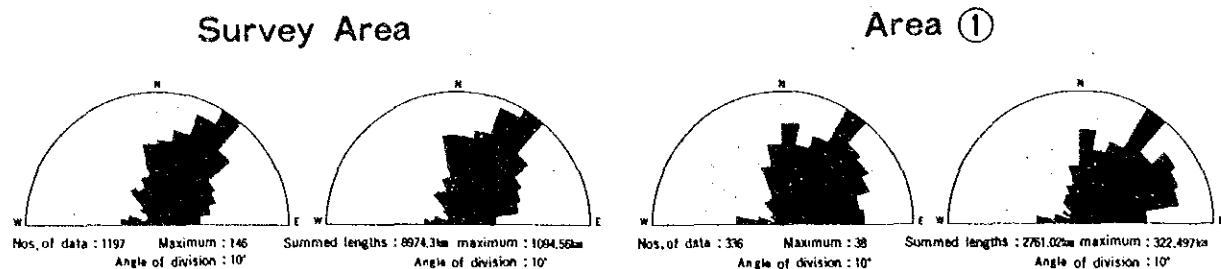


Fig. II 1.1 Main tectonic block and radial diagrams for lineament of each geological block

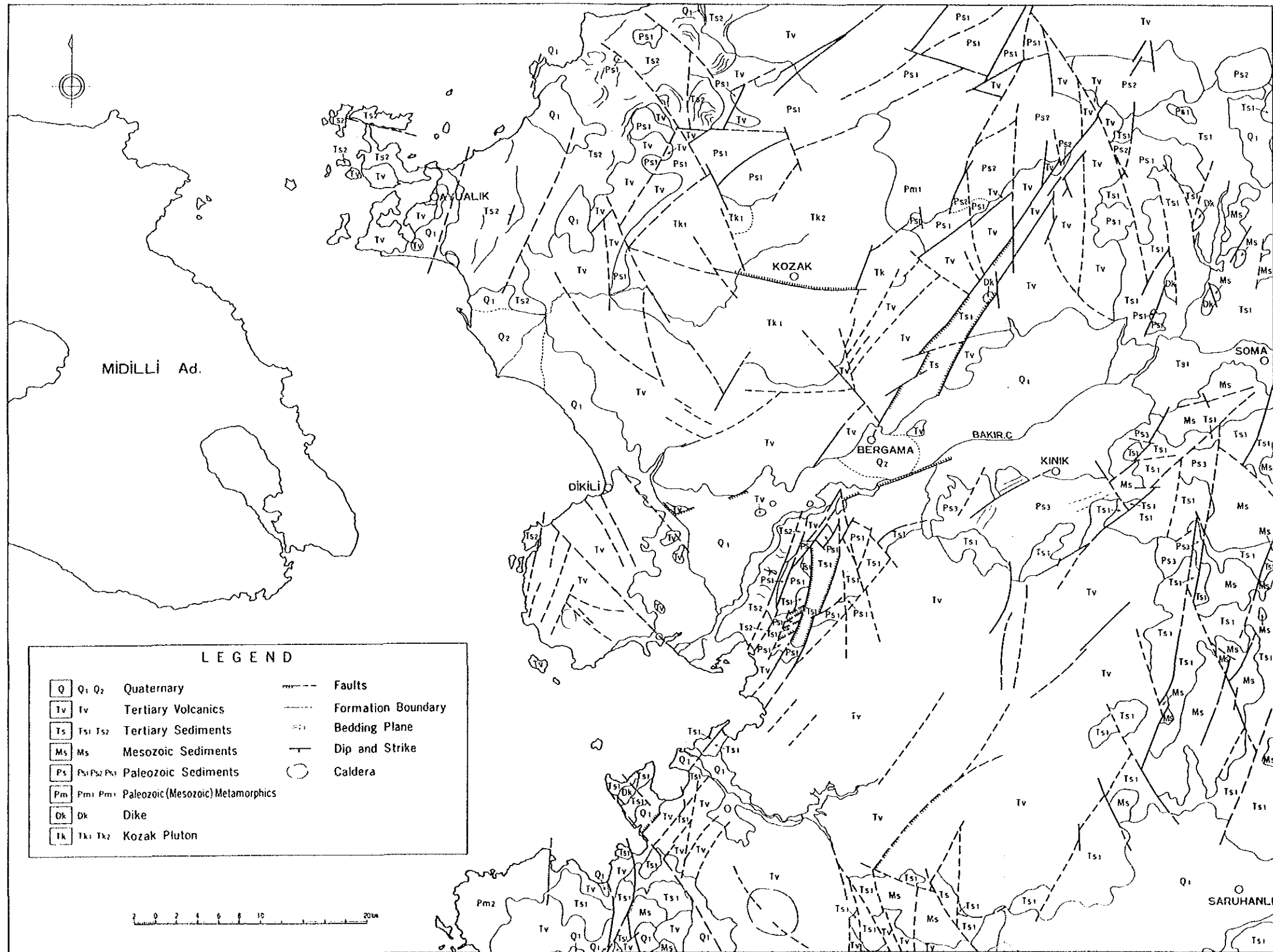


Fig. II.1.2 Geological interpretation map from Landsat image



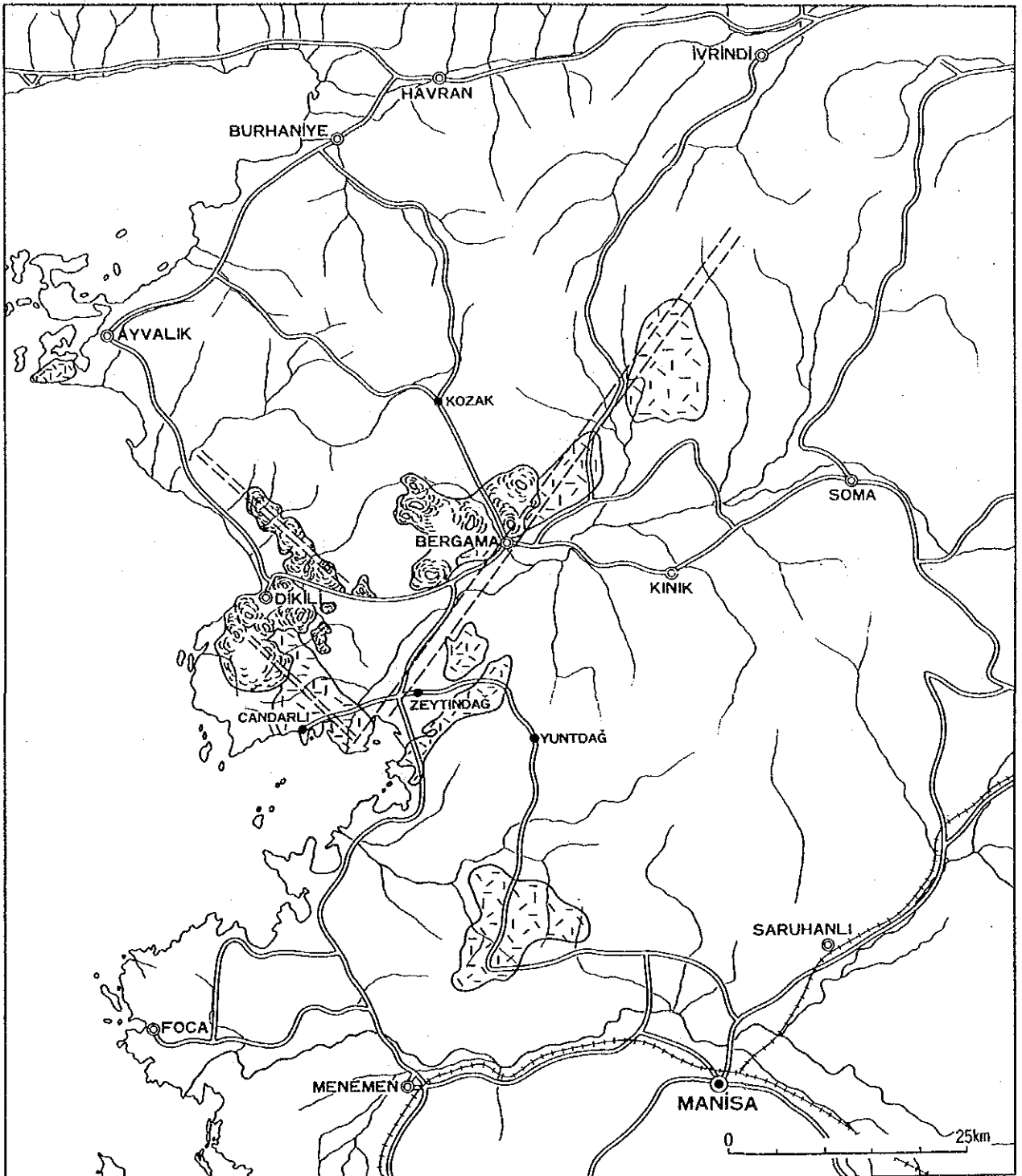


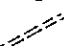


Fig. II.1.3 Distribution map of pyroclastic rocks (Tp) and youngest Yuntdağ volcanics (Tyu<sub>3</sub>)

-  Pyroclastic rocks (Tp)
-  Youngest Yuntdağ volcanics (Tyu<sub>3</sub>)
-  Fractured zone

The geology of the dikili-Bergama area and its surroundings has been classified into 14 units in Fig. II.1.2.

## (2) Interpretation of aerial photographs

Lineament, topography and geothermal manifestations on the aerial photographs of 1 : 35,000 scale were investigated in detail with the aid of Landsat images interpretations. The main trends of lineaments is N50°W. N30°–40°E trending lineaments are observed as shown in Fig. II.1.4. Characteristics of texture of altered zones represent that the drainage irregularity is densified in argillaceous zone and that the rugged outcrops develop in silisified zones.

## 3. Geological reconnaissance

The geology of Dikili-Bergama is made up the basement rocks, Kozak pluton, Yuntdağ volcanics I, Soma formation, Pyroclastic rocks, Yuntdağ volcanics II, Yuntdağ volcanics III, Dededağ basalt and Alluvium in Fig. II.1.5 and Table II.1.1.

The pre-Tertiary basement rocks are made up of the Camoba on Kınık formations around the Kozak mountains. The former comprises siltstone and silty limestone of Permianage. The latter is composed mainly of mudstone and limestone of Triassicage. These are thought to be distributed at a great depth in the region from Dikili to Bergama.

The Kozak pluton is composed of the granodiorites which are exposed in the northeast of the survey area. The results of radiometric age determination show that the rocks intruded during Eocene time to Oligocene time.

The Yuntdağ volcanics I are widely distributed in the southwestern part of the Kozak mountains. They consist of various kinds of andesite varying from pyroxene andesite to dacite. The rocks are often strongly altered.

The Soma formation is distributed in the eastern part and south-western part of the survey area. It consists of sandstone, siltstone, silty limestone and large amounts of tuffaceous sediment. At the same time, the depression movement which led to the deposition of this formation is probably related to the volcanic activity of felsic magma.

The Yuntdağ volcanics II form Yuntdağ mountain which consists of horn-



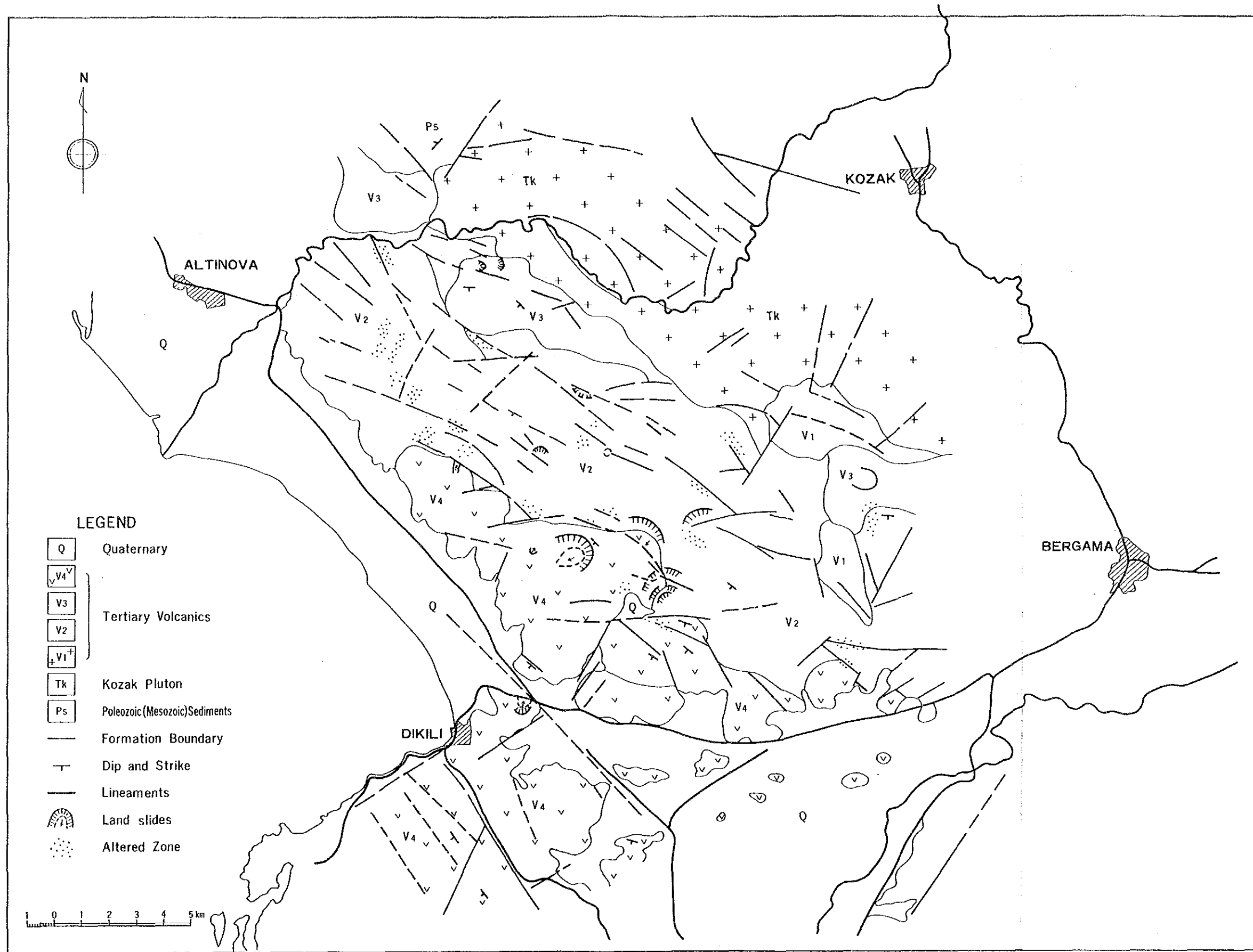
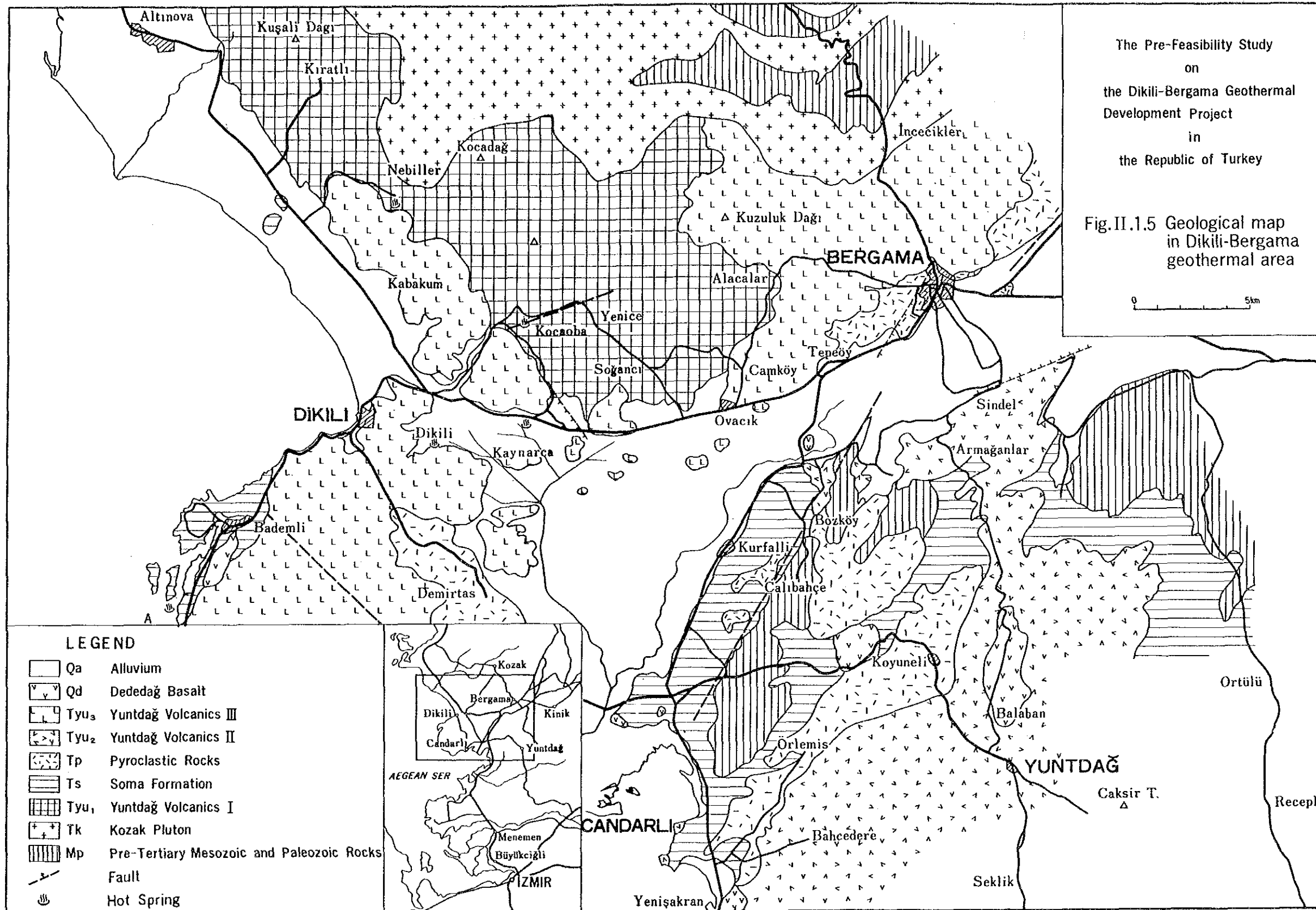
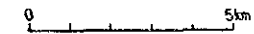


Fig. II.1.4 Geological interpretation map from aerial photographs.

The Pre-Feasibility Study  
on  
the Dikili-Bergama Geothermal  
Development Project  
in  
the Republic of Turkey

Fig.II.1.5 Geological map  
in Dikili-Bergama  
geothermal area



LEGEND

- Qa Alluvium
- Qd Dededağ Basalt
- Tyu<sub>3</sub> Yuntdağ Volcanics III
- Tyu<sub>2</sub> Yuntdağ Volcanics II
- Tp Pyroclastic Rocks
- Ts Soma Formation
- Tyu<sub>1</sub> Yuntdağ Volcanics I
- Tk Kozak Pluton
- Mp Pre-Tertiary Mesozoic and Paleozoic Rocks
- Fault
- Hot Spring

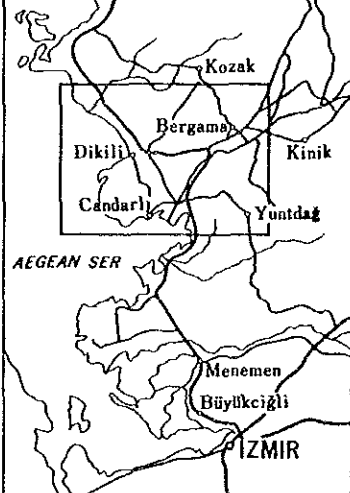
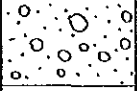

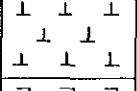
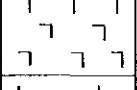
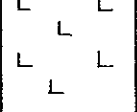
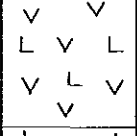

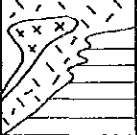
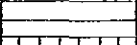

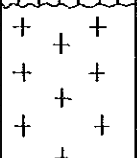
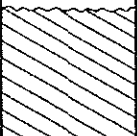




Table II 1.1 Geological succession of the Dikili – Bergama geothermal area

Age		Geologic Column	Rock Name	Remarks	
Quaternary	Holo-cene		Alluvium	Mud, Sand, Gravel	
	Pleisto-cene		Dededag Basalt (Od)	Basalt, Pyroxene Andesite	
Tertiary	Pliocene			Rhyolite	Post Volcanism is a heat source of the present geothermal activity
			Yuntdag Volcanics III (Tyu <sub>3</sub> )	Dacite	
				Biotite - Hornblende Andesite	
	Pliocene		Yuntdag Volcanics II (Tyu <sub>2</sub> )	Basalt, Pyroxene Andesite	
				Hornblende Andesite, Pyroxene Andesite	
	Eocene ~ Miocene		Pyroclastic Rocks (Tp)	Felsic Pyroclastics, Ignimbrite, Dacite lava	A cap rock of geothermal reservoir
			Some Formation (Ts)	Limestone, Tuffaceous mudstone, Silts tone	
Eocene ~ Miocene		Yuntdag Volcanics I (Tyu <sub>1</sub> )	Hornblende Andesite, Biotite bearing Hornblende Andesite	Fracture zone is probably an aquifer	
		Kozak Pluton (Tk)	Granodiorite		
Pre - Tertiary		Pre - Tertiary Basement Rocks (Mp)	Camoba Formation Kınık Formation		

blende andesites and pyroxene andesites. The Yuntdağ volcanics III forms lava domes and are situated in the Dikili area and in the northwest of Bergama. They consist mainly of biotite-hornblende andesite and dacite.

The Dededağ basalt outcrops locally in the Dikili-Bergama basin. The rock consists of dark gray, compact lava flows of pyroxene andesite and basalt. The Dededağ volcano is thought to have formed in early Pleistocene time.

The Dikili-Bergama area is characterized by a NE-SW trending fracture zone which runs from the south of Bergama. Many NW-SE faults are inferred to form a small graben.

#### 4. Preliminary geochemical survey

In the Dikili-Bergama geothermal area, there are more than 20 hot springs as shown in Fig. II.1.6. Using existing data on temperature and the chemical composition of hot springs, 18 water samples of the hot springs were collected in Fig. II.1.7. Surface waters were also collected for isotope analysis.

In the survey area, there is a high possibility that geothermal fluid is reserved in a fracture zones in the Yuntdağ volcanics I and pre-Tertiary limestone. Hot waters from hot springs, except for the Bademli hot spring are considered to be of meteoric water origin from isotope analysis.

Hot water from most hot springs is of neutral-weakly alkaline Na-HCO<sub>3</sub> or SO<sub>4</sub> type (Fig. II.1.8). The Kaynarca hot spring seems to be derived from a reservoir of temperature higher than 180°C in this area. Considering the fact that HCO<sub>3</sub>(-SO<sub>4</sub>) type hot water discharging in the Dikili and Kaynarca hot springs has reacted with reservoir rock in Fig. II.1.9, there may be high temperature reservoir at depths. Fig. II.1.10 shows that the geochemical temperature of the Kaynarca hot spring is the highest, exceeding 180°C. Therefore, the Dikili-Kaynarca area is judged to be the most prospective area from the geochemical data.

#### II.1.2 Regional geological structure and geothermal activity

In the south-western Anatoria, the E-W trending graben was formed, resulting from a NNE-SSW oriented tensional stress field and the following E-W compressional stress field.

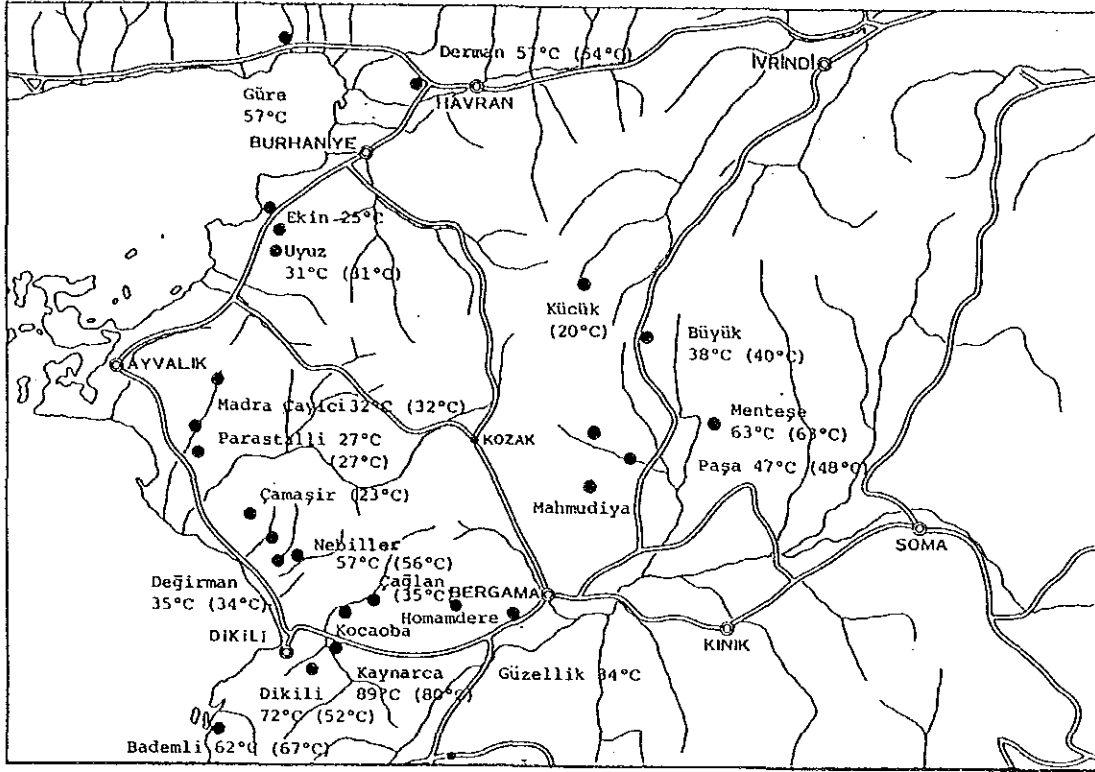
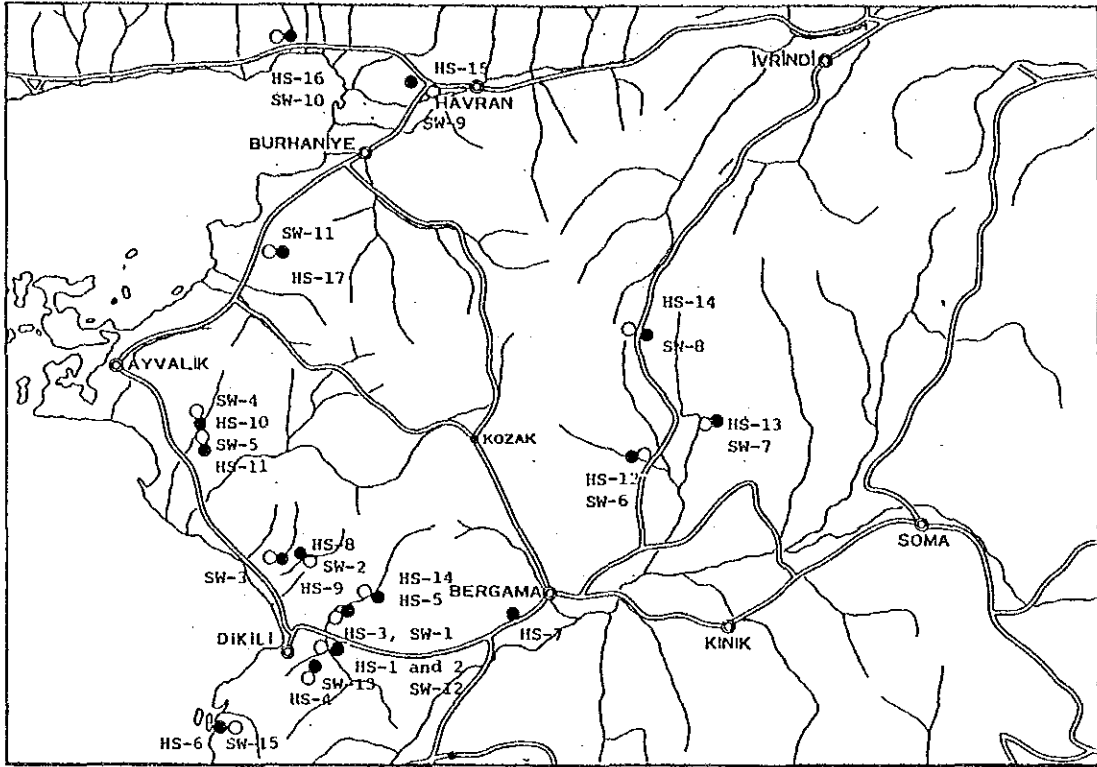


Fig. II.1.6 Location and measured temperature of hot springs in the Dikili-Bergama geothermal field (Values in parentheses are temperatures of hot springs reported by S. YILMAZER)



● : Hot water  
○ : Surface water

Fig. II.1.7 Sampling sites of hot spring waters in the Dikili-Bergama geothermal field.

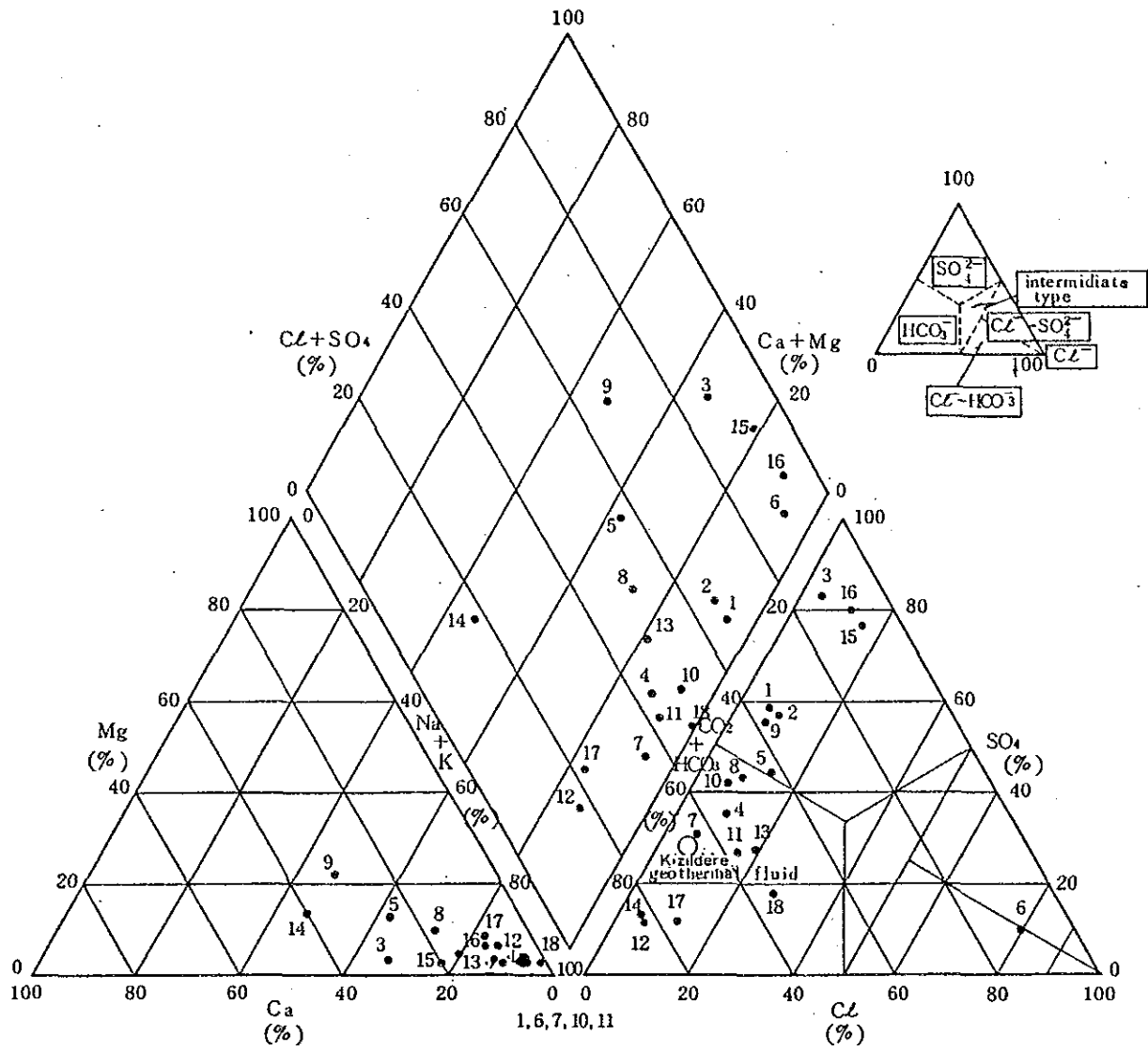


Fig. II.1.8 Piper tri-linear plots of hot springs in the Dikili-Bergama geothermal field



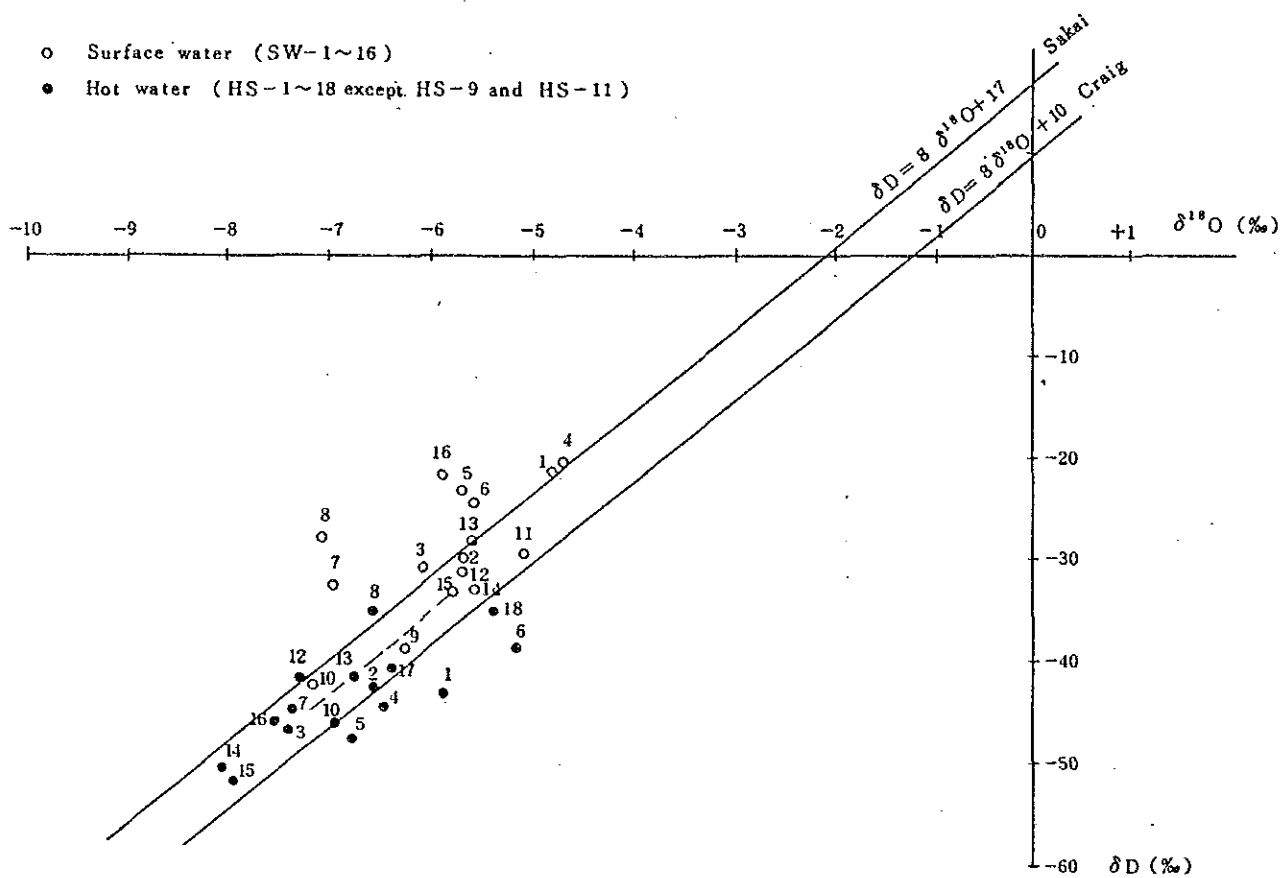


Fig. II.1.9 Deuterium and oxygen-18 isotope ratios of hot spring and cold water (surface water) in the Dikili-Bergama geothermal field.

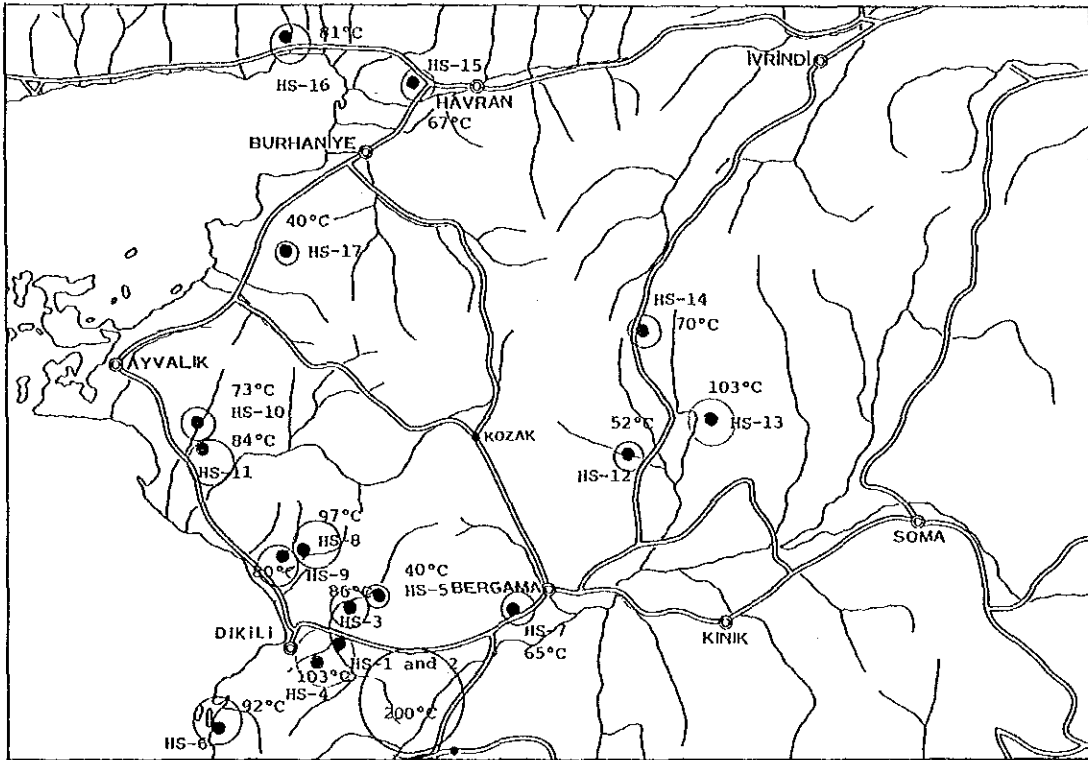


Fig. II.1.10 Reservoir temperature calculated by using silica thermometer in the Dikili-Bergama geothermal field.



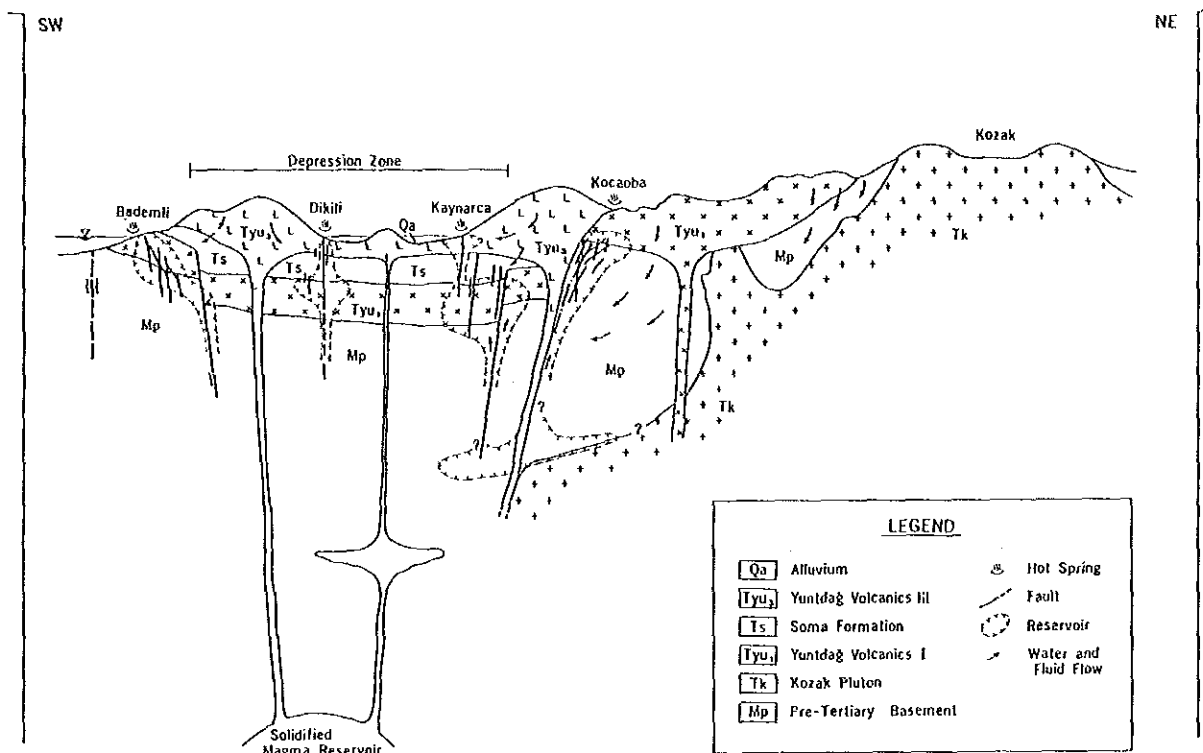


Fig. II.1.11 Conceptual model of Dikili-Bergama geothermal area



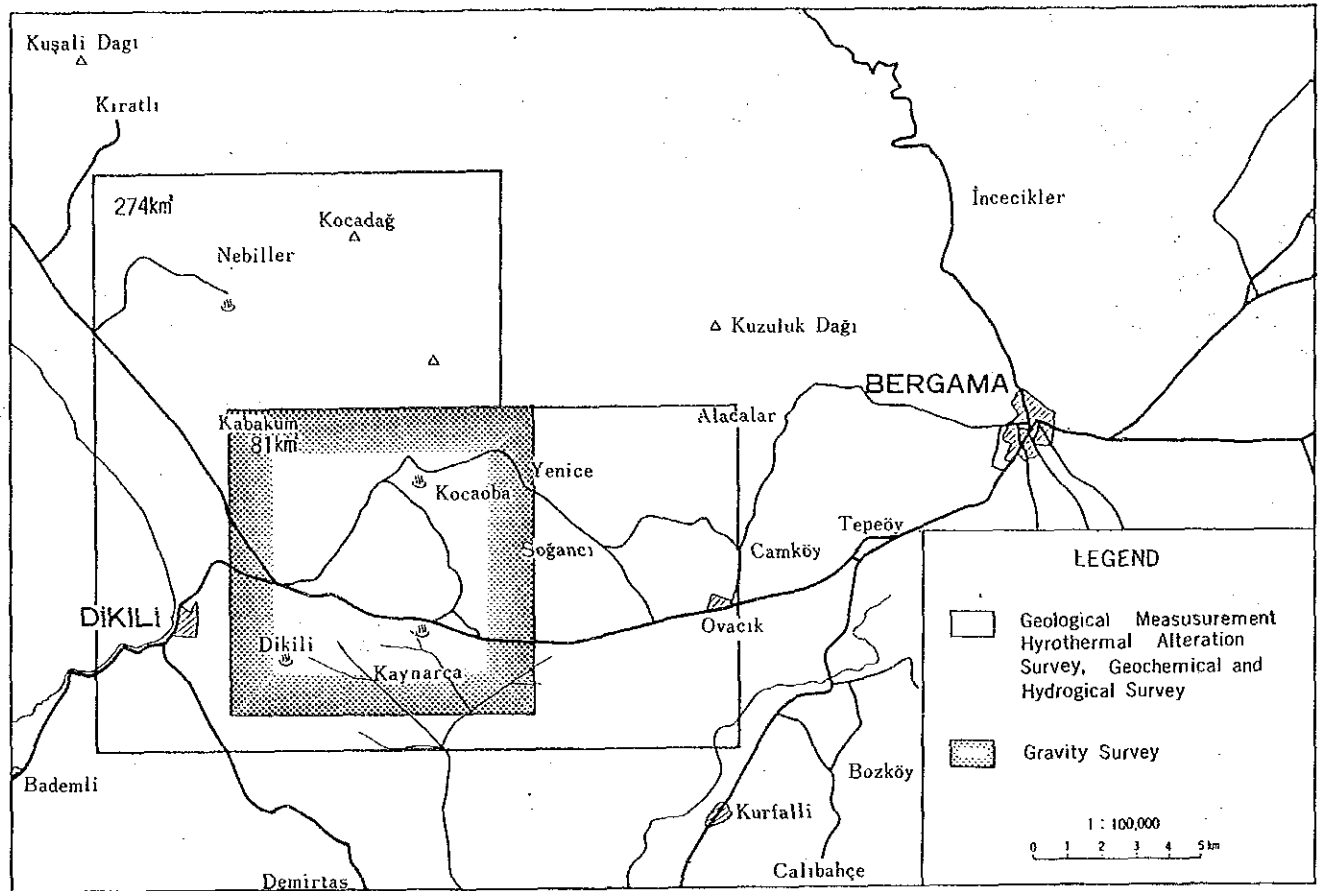


Fig. II.1.12 Survey area for second stage exploration.



Based on the gravity anomaly, it is assumed that there is a long depression zone from Bergama to Dikili. The results of the geological survey support the existence of E-W and NW-SE trending grabens. Besides a long and narrow graben with NE-SW trend was observed in the east.

The Dikili-Bergama geothermal area became a site of volcanism during Tertiary time and early Quaternary. To the north of Dikili, dome shaped volcanoes from late Pliocene time to early Pleistocene time are formed along NE-SE trending fault. Around these volcanoes, geothermal manifestations such as relatively high temperature springs, travertine and altered zones are distributed. Therefore, the heat source of geothermal activity in the Dikili-Bergama area is caused by the post volcanism. It is certain that heat is probably derived from magmatism and radioactive decay of Kozak granodiorite.

In the survey area, hot springs are distributed around the Kozak pluton. In particular they are concentrated in the southwest and southeast of the pluton. As mentioned above, the Kaynarca hot spring which has the highest temperature of 89°C is distributed in the lowland between the Yuntdağ III volcanoes and on the E-W trending faults. The faults were determined from gravity anomaly data. Other hot springs with a temperature higher than 60°C are situated at Dikili (72°C), Kocaoba (62°C) and Menteşe (63°C) shown in Fig. II.1.6.

The Bedemli hot spring which is situated on the seashore 5 km south from Dikili is fed by local fractures in the Yntdağ volcanics I (T<sub>yu1</sub>). It shows that hot water tends to be reserved in its fracture zone.

### II.1.3 Conceptual model

From the results of the first stage exploration, the conceptual model of the Dikili-Bergama geothermal area could be drawn in Fig. II.1.11. In this area, the E-W extending lowland seems to result from a graben structure. Moreover, small grabens formed in the same direction as the NW-SE trending faults before the eruption of the Yuntdağ volcanics III.

Reservoirs are expected in the fracture zones which are developed in the Yuntdağ volcanics I, pre-Tertiary limestone and a boundary of Kozak pluton and pre-Tertiary basement rocks. The Soma formation forms the cap of the reservoirs. It is considered that the reserved hot-water is meteoric water in origin, which recharged in high mountain land such as the Kozak massif and is heated at depth.

Geothermal fluid probably comes up through the E-W and NW-SE trending faults which form the graben, and discharges in Kaynarca, Dikili Ilıcasi and Kocaoba.



The chemical characteristics of the reservoir fluid is of neutral-weakly alkaline  $\text{HCO}_3$  ( $\text{SO}_4$ ) type and the temperature of the deep reservoir is estimated to be more than  $180^\circ\text{C}$ .

#### **II.1.4 Selection of the prospective area for the second stage exploration**

According to the above results on delimitation of the prospective geothermal area, the survey area for the next stage was selected as shown in Fig. II.1.12. The area of  $274 \text{ km}^2$  covers the Nebiller, Kocaoba, Dikili and Kaynarca hot springs.

### **II. Outline of the second stage exploration**

#### **II.2.1 Summary of survey results**

The second stage exploration was carried out in an area of  $274 \text{ km}^2$  which was estimated after the first stage exploration. In this stage, the most prospective area was selected on the basis of the results of geological measurement, hydrothermal alteration survey, geochemical and hydrological survey and gravity survey.

##### **1. Geological measurement**

Using rock samples collected from each formation, the rock name and rock type were confirmed and the rock property and rock age were measured. The relationships found between the physical rock properties are as follows:

- a strong negative correlation between the porosity and density,
- as the porosity increases, the thermal conductivity, magnetic susceptibility and resistivity tend to be lowered,
- weak positive correlations among the thermal conductivity, magnetic susceptibility and resistivity,
- the magnetic susceptibility increases as the rocks become more mafic.

The role of each formation in the geothermal model is as follows:

##### **(1) Pre-Tertiary rocks, Kozak pluton and Yuntdag volcanics**

The rocks are not very permeable in themselves, but it is presumed that continuous fractures at deep subsurface are probably formed along faults.

The fracture zone may allow the passage of hot water or form a geothermal reservoir itself.

## (2) Soma Formation and Pyroclastic rocks

The rocks possibly play a role of reservoirs on account of their high porosity, more than 30 percent. The formation is ductile under stress which makes it difficult for continuous fractures to develop. Accordingly it is thought that the rocks act as a sealing bed in the geothermal system. Moreover, the absolute ages of the volcanic rocks in this area are old and it is unlikely that the igneous activities related to existing geothermal activity.

## 2. Hydrothermal alteration survey

In this survey, 59 samples of altered rocks were analyzed by X-ray powder diffraction method and 20 samples of these were analyzed chemically. From the results of the field survey and X-ray analysis, hydrothermal alteration is divided into the following four types: silica mineral type, alunite type, kaolin-pyrophyllite type, alumino-clay type and zeolite-alkalifeldspar type.

Based on the results of hydrochemical alteration survey, the relationship between alteration and the geological structure and between alteration and the geothermal activity were discussed. In addition, the homogenized temperature of fluid inclusions of quartz vein was measured to estimate the reservoir temperature.

As shown in Fig. II.2.1, altered zones are distributed in the following five areas:

- (1) Salihler-Gökçeayıl area
- (2) Kocaoba area
- (3) Sağancı-Ovacık area
- (4) Kaynarca area
- (5) Dikili Ilıca area

Of these, the outcrops of mostly and wholly altered rocks extend approximately 18.5 km<sup>2</sup> in total. Hydrothermally altered zones are composed of

- (1) silica minerals; tridymite, cristobalite opal and quartz,
- (2) clay minerals; kaolin, montmorillonite, mixed layer mineral and chlorite,
- (3) other minerals; alunite, gypsum, calcite and pyrite.

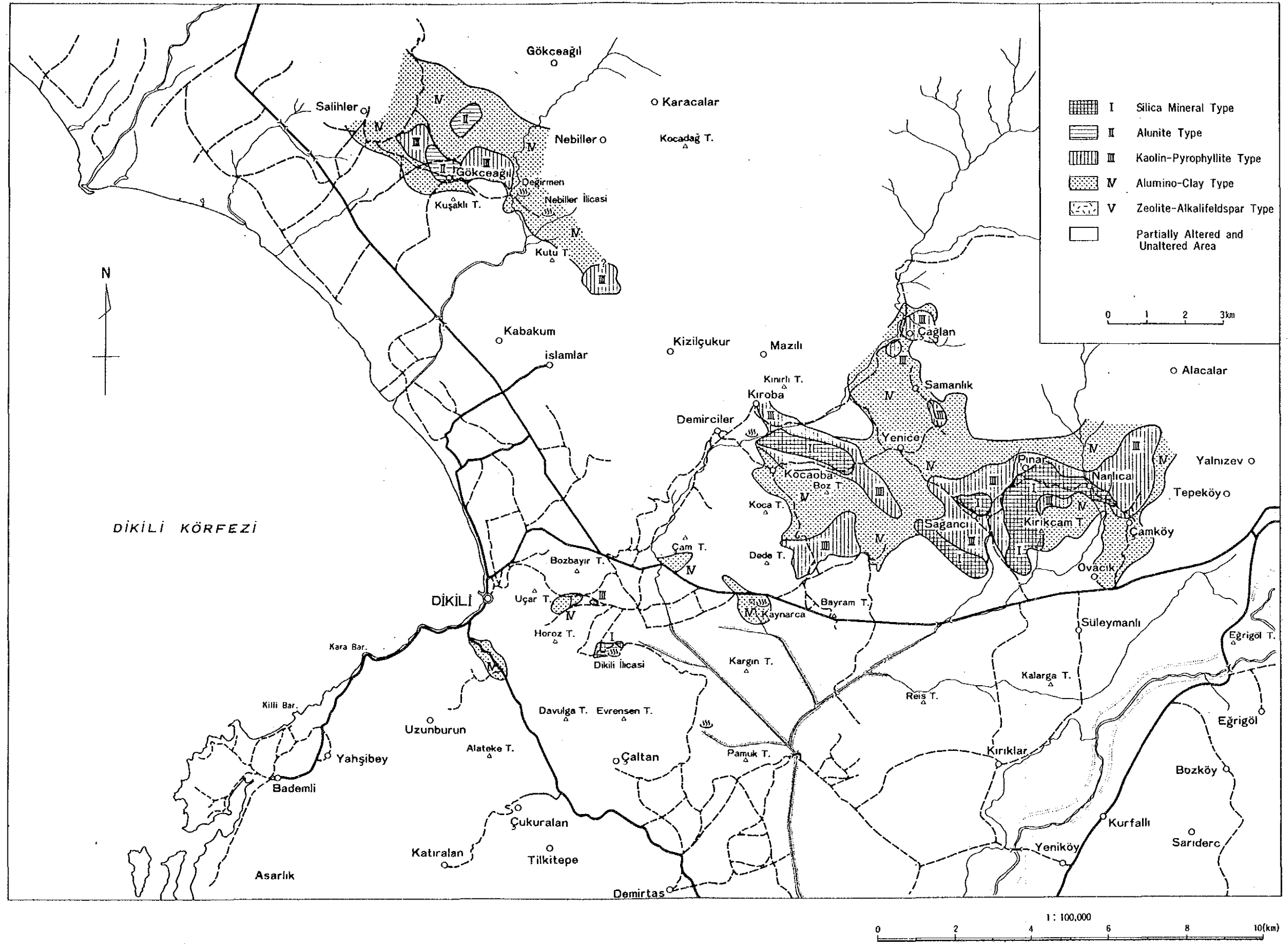


Fig. II.2.1 Alteration zone map



In the Kaynarca area which is geothermally the most active, the altered zones are characterized by quartz, alphas-cristobalite, calcite associate with montmorillonite and mixed layer minerals.

As to the reactivity of the chemical component during the alteration, it was made clear that  $K_2O$  and S mostly concentrate and/or remain in rocks. On the other hand, the components such as  $MgO$ ,  $CaO$  and  $N_2O$  are mostly leached out from rocks.

In the north and northeastern part of the study area, altered zones extend from NW to SE. Especially, silicified altered zone and hydrothermal mineral veins of quartz and calcite are distributed along NW-SE trending fault. Accordingly, it was concluded that these faults are vertical conduits for geothermal fluid. Alteration in the survey area can be divided into the following three stages:

- (1) Before sedimentation of the Some Formation
- (2) Before Yuntdağ II volcanism
- (3) After Yuntdağ III volcanism

Before the sedimentation of the Soma Formation, the hydrothermal alteration acted chiefly from Kocaoba to Sağancı in the east of the survey area. The alteration resulted from geothermal activity of which the magmatism of Yuntdağ Volcanics I was the heat source. The acting fluid in this stage is probably of a neutral-facidic condition of pH and the temperature exceeds  $150^{\circ}C$ .

In the northern part of the survey area, Demirtaş Pyroclastic rocks had undergone hydrothermal alteration. The altered zone was formed in Miocene time to Pliocene time and resulted from the geothermal activity associated with the felsic magmatism. It is inferred that the geothermal fluid in this stage is strongly acidic and its temperature is relatively low.

Since weakly altered zones in the Kaynarca area occur in the latest Yuntdağ Volcanics III, the alteration seems to be related to the present geothermal activity seen at Kaynarca, Kocaoba and Dikili Ilıcasi hot-springs. Consequently, there is a possibility that the post volcanic action of the latest volcanism of the Yuntdağ Volcanics III is the heat source of the present geothermal activity.

### 3. Geochemical and hydrological survey

The hydrological survey (hydrogeochemistry) and the geochemical survey (soil and soil-gas surveys) were carried out by chemical analysis (22 hot water

samples) and isotopic analysis (10 hot water samples and 24 cold water samples) and chemical analysis of soil and soil-gas (302 samples), respectively. The chemical and isotopic data, characteristic of the geothermal system, chemical characteristics of subsurface fluid, reservoir fluid temperature, discharging zone of geothermal fluid and so on are discussed in the following section.

- (1) The isotope data show that the origin of the hot waters discharging from the Kaynarca, Dikili Ilıcasi and Kocaoba hot-springs must be of meteoric water. Hot water discharging from these hot springs is considered to be mixture of waters of various chemical characteristics as described later. The main constituent water in the hot water from Kaynarca and the Dikili Ilıcasi seems to be common and derived from the same deep reservoir (this geothermal system spreaded out in and around the Kaynarca area is termed "the Dikili-Kaynarca system"). The geothermal system is considered fundamentally to be of water-dominated type determined by the chemical composition of hot water. The subsurface fluid seems to be mainly composed of neutral  $\text{HCO}_3$  type water.
- (2) The chloride ion in the hot water of the Dikili-Kaynarca geothermal system must originate from sea-water or deep geothermal water. The fluid of the Dikili-Kaynarca system consists of  $\text{HCO}_3$ (- $\text{SO}_4$ ) type water and water containing relatively rich-Cl.

Bubbling gas composed of  $\text{CO}_2$  as a major component in the hot springs and  $\text{HCO}_3$ -rich hot water indicate very high  $\text{PCO}_2$  and high  $\text{HCO}_3$  concentration in the reservoir, which is probably in equilibrium with calcium carbonate originating from decomposition of organic materials in sedimentary rocks from the delta-13C values

- (3) The water recharged to deep level in the Dikili-Kaynarca system is inferred to be heated mainly by thermal conduction of rocks, because it does not contains magmatic fluid. The heat source of the Dikili-Kaynarca system, however, seems to be related to magmatism, from the helium isotope data of the Dikili Ilıcasi hot-springs.
- (4) The reservoir temperatures of  $\text{HCO}_3$  (- $\text{SO}_4$ ) type water discharging mainly from the Kaynarca hot-spring is estimated to be 180 to 200°C and from Dikili Ilıcasi is 110 to 160°C. The temperature of the deep reservoir is assumed to be 220 to 230°C from the isotope temperature of  $\text{SO}_4$ - $\text{H}_2\text{O}$ .

- (5) There is a boiling hot spring at Kaynarca. The Dikili-Kaynarca geothermal system is of water-dominated type. Therefore, the maximum temperature of geothermal fluid in fractures along faults in Kaynarca is considered to be controlled by the boiling point at each depth. If the reservoir fluid contains abundant CO<sub>2</sub> gas, boiling temperature of this fluid becomes considerably lower than that of pure water. Therefore, the HCO<sub>3</sub> (-SO<sub>4</sub>) type fluid of about 200°C must be reserved at a considerable depth due to a relatively high CO<sub>2</sub> content.
- (6) Based on the delta-D values of each hot spring, the recharge areas of these springs, namely the Dikili Ilıcasi, Kocaoba and Kaynarca hot-springs, are considered to be approximately in the same area. The meteoric water recharges around the southern slope of the Kozak massif, and migrates to the southwest, as shown in Fig. II.2.2. The circulation time of the water discharging at Dikili Ilıcasi and Kaynarca are concluded to be more than 75 years. The water discharging at Kocaoba is considered to be younger (46 year) than the water at Kaynarca and Dikili Ilıcasi.
- (7) Based on the results of the geochemical survey (analysis of Hg, CO<sub>2</sub> and Rn in soil-gas and analysis of Hg in soil), the up-flow zone of geothermal fluid in and around the Kaynarca hot spring and the tectonic lines which allow the passage of geothermal fluid were inferred as shown in Fig. II.2.3.
- (8) According to the chemical characteristic of the boiling hot spring at Kaynarca, it is feared that carbonate scale problems will occur during the development of the Dikili-Kaynarca system.

#### 4. Gravity survey

The gravity survey was carried out at 693 stations at about 300 m interval in the 81 km<sup>2</sup> study area. The data was processed to prepare Bouguer anomaly map, residual gravity map and the two-dimensional section.

As shown in Fig. II.2.4 and Fig. II.2.5, the pattern of the gravity distribution is described by four major anomalies, two low gravity zones and two high gravity zones. The two low gravity zones which are located at the north-western and southeastern parts correlate with the lithology and geological structure. On the other hand, the high gravity zones which are recognized at the northeastern and southwestern parts roughly correlate with the extent of Yuntdağ volcanics I. The southwestern positive anomaly shows that pre-

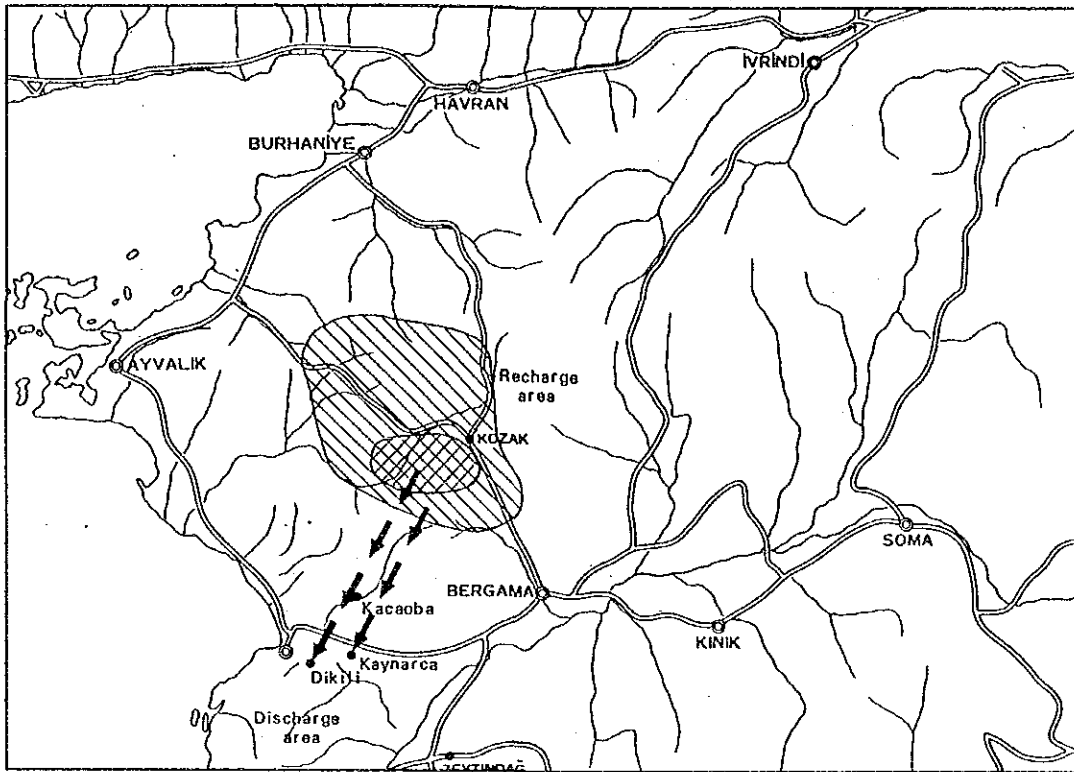
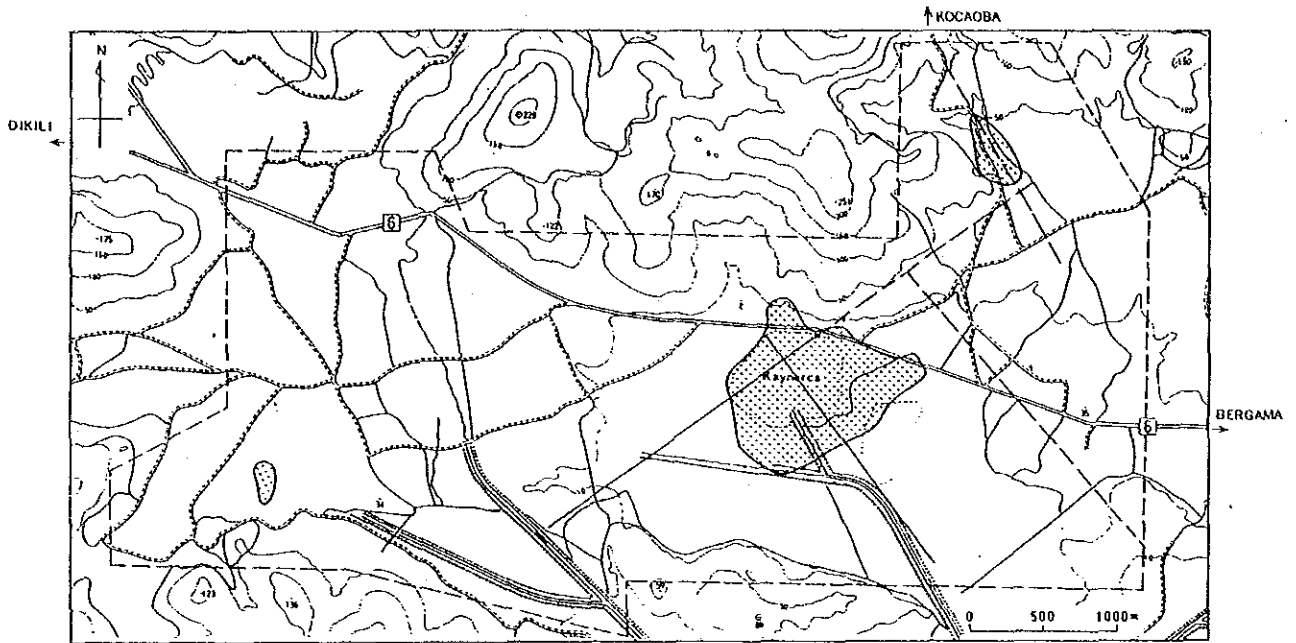


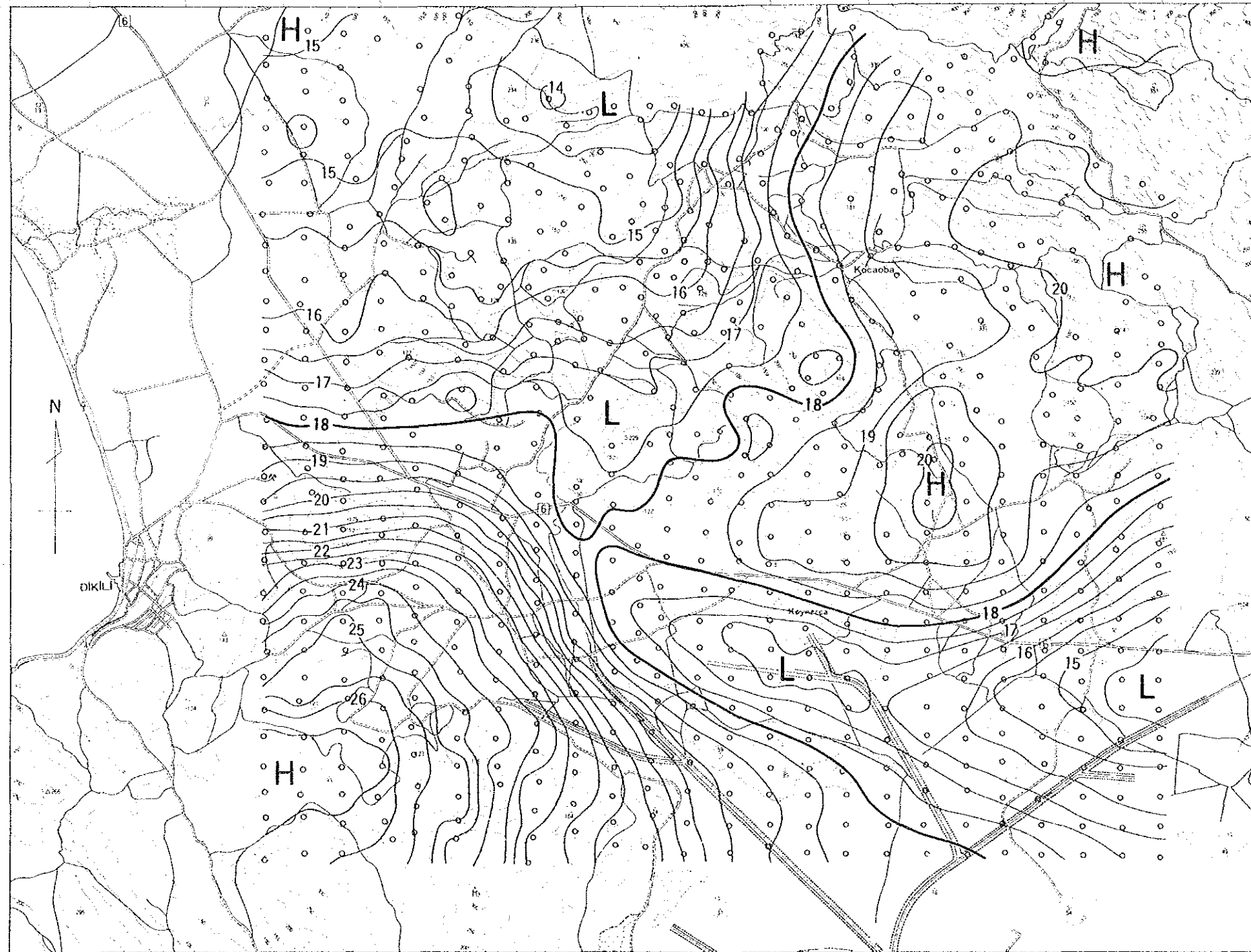
Fig. II.2.2 Fluid flow pattern of the Dikili – Kaynarca system





- ⊙ : Overlapped area of high Hg contents in soil and soil-gas
- : Tectonic line estimated from Hg distributions in soil and soil-gas
- - : Tectonic lines estimated from Hg distribution in soil

Fig II 2.3 Tectonic lines in relation to geothermal activity

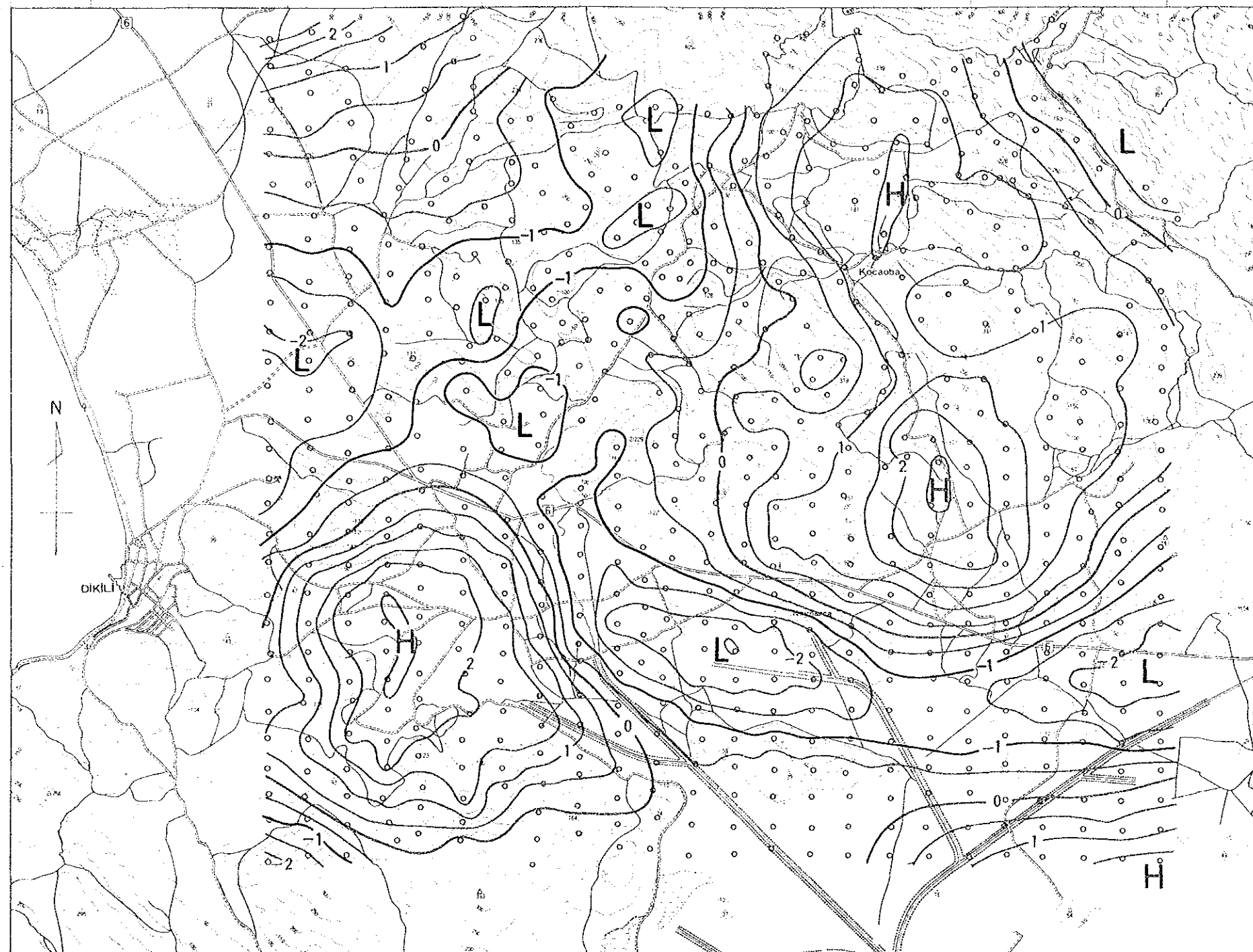


JAPAN INTERNATIONAL COOPERATION AGENCY — GENERAL DIRECTORATE OF MINERAL RESEARCH AND EXPLORATION

GEOHERMAL DEVELOPMENT PROJECT  
IN  
DIKILI-BERGAMA FIELD

0 1 2 3(km)

Fig. II.2.4  
Detailed bouguer anomaly map  
( $\rho=2.4$ )



JAPAN INTERNATIONAL COOPERATION AGENCY — GENERAL DIRECTORATE OF MINERAL RESEARCH AND EXPLORATION

GEOTHERMAL DEVELOPMENT PROJECT  
IN  
DIKILI-BERGAMA FIELD

0 1 2 3 (km)

Fig. II.2.5  
Detailed residual gravity map  
( $\rho=2.4$ )



Tertiary basement is undoubtedly uplifted near the surface.

In the southeastern part of the survey area, the WSW-ESE trend of the contour distribution and the shape of the low anomaly seems to reflect faults and grabens. The low gravity anomaly in the southwestern part is correlated with the distribution of the Soma formation and felsic pyroclastic rocks. There is no obvious relationship between the gravity anomaly and the distribution of the Yuntdağ volcanics III.

Based on the result of the two-dimensional section analysis, there is a possibility that the low gravity zone at the south of Kaynarca represents alluvium of 200 to 300 m in thickness.

### II.2.2 Subsurface geological structure

In the second stage survey area, pre-Tertiary rocks and the Kozak platon presumed to be distributed in the subsurface, because these basement rocks crop out in Kozak massif, in the northeastern part of the survey area. As shown in Fig. II.2.6, and Fig. II.2.7, the survey area is characterized by NW-SE trending faults. Of these, the fault from the Kocaoba hot spring through Sağancı to Ovacık can be traced. Since a silicified zone and a hydrothermal mineral vein occur along the fault in the Yuntdağ volcanics III, the fault presumably extends to great depth. Two NW-SE trending faults which run through Kocaoba in the north and through Dikili Iıcasi in the south form a graben. Moreover, the zone between the E-W trending fault through Kaynarca and the NW-SE trending fault through Dikili Iıcasi is considered to be a graben on the basis of the low gravity anomaly and geological data.

On the other hand, there may be a horst because Yuntdağ volcanics I outcrop from Dikili to Demirtas. Judging from the high gravity anomaly in the southwestern part of the survey area, intrusive rock from younger magmatism seems to form a horst.

As mentioned above, it is inferred that there are small horsts and grabens of 2 to 5 km width of pre-Tertiary basement and Yuntdağ volcanics I, resulted from NW-SE trending fault movement.

High temperature hot springs with temperature greater than 60°C are located on the faults which forms the graben.

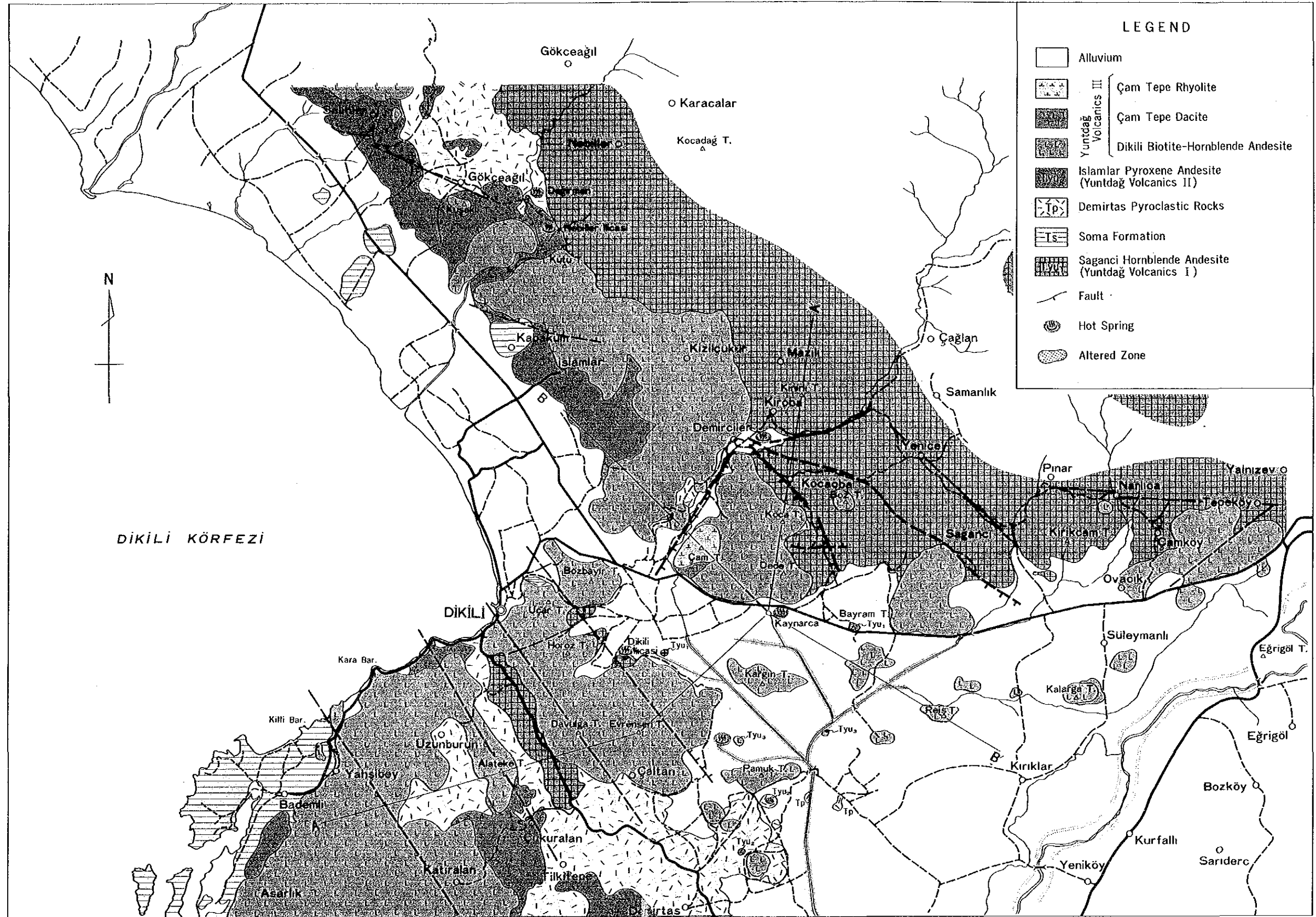


Fig. II.2.6 Geological map of Dikili-Ovacık area

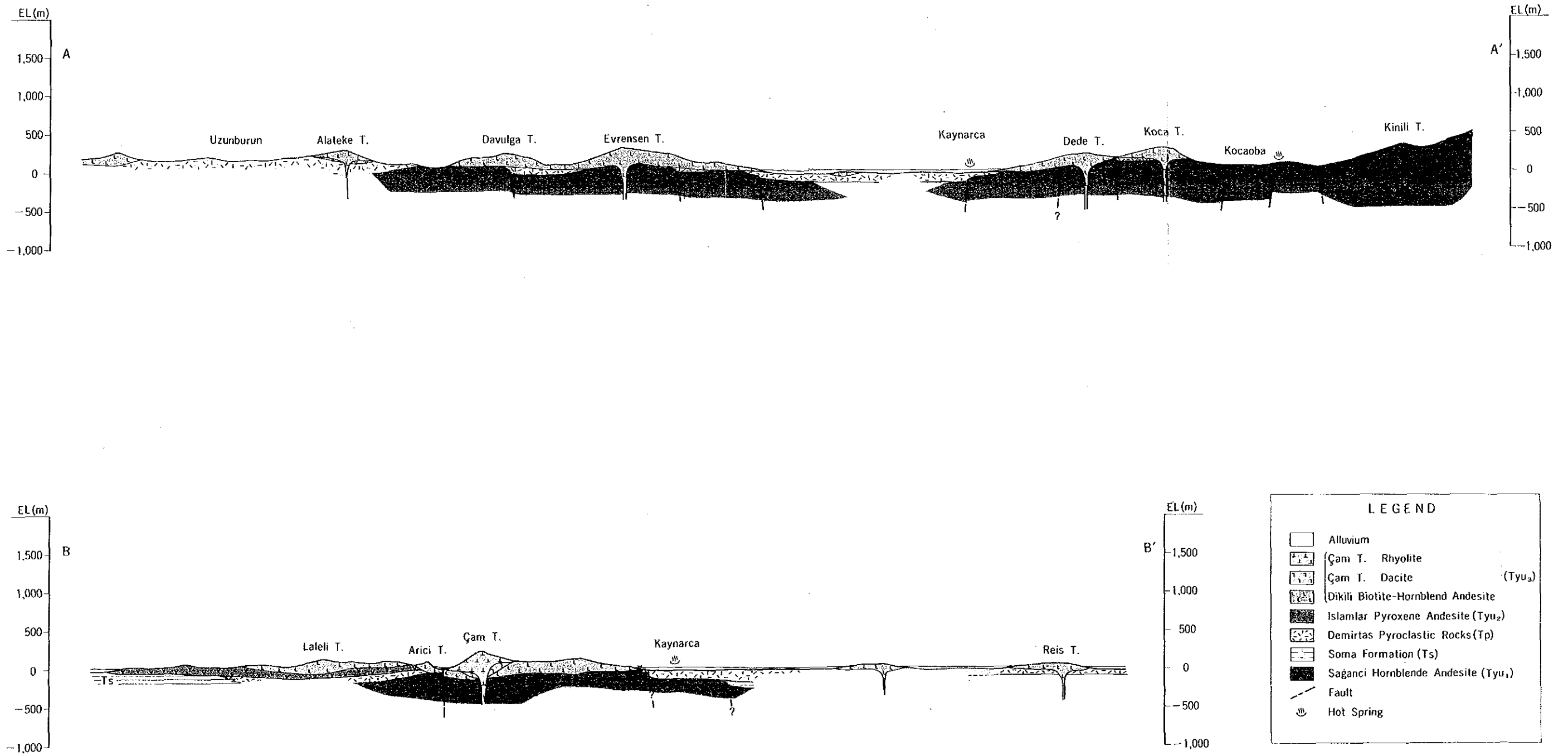


Fig. II.2.7 Geological cross section of Dikili-Ovacik area.





### II.2.3 Volcanism and history of geothermal activity

In the Dikili-Bergama geothermal area, intense volcanism took place after the intrusion of the Kozak granitic magma of Tertiary age. The volcanic activity increased in intensity in Miocene time and continued during Pliocene time. There were four main volcanisms during Neogene time as follows; andesite volcanism of Yuntdağ Volcanics I, felsic volcanism of Demirtas Pyroclastic Rocks, mafic volcanism of Yuntdağ Volcanics II and dacite volcanism of Yuntdağ Volcanics III.

The andesite volcanism took place in the center of the southwestern slope of the Kozak massif. The volcanic activity erupted chiefly hornblende andesite which were about 1,500 meters in maximum thickness. Around Nebiller village in the north-western part of the survey area, porphyritic rocks are widely distributed. From the results of the absolute age determination, the rocks are thought to be 15 to 16 Ma, which presumably erupted during Miocene time.

The following felsic volcanism took place and an enormous thickness felsic pyroclastic rocks accumulated during the later stage of sedimentation of the Soma formation. The activity center of the volcanism is probably situated in Demirtas, in the southwestern part of the survey area, where a low gravity anomaly is recognized. The absolute age shows 13 to 15 Ma. Uplift in the region was accompanied by the felsic magmatism. In the same field of the felsic magmatism, the mafic magma flowed out. That is, early violent eruptions producing welded ash flow gave way, with the loss of volatiles, to quieter eruption producing mafic lava flows.

From the existing data, some parts at least of the mafic rocks such as pyroxene andesite and basalt were correlated with dededag basalt of the Quaternary. They, however, are locally capped by the Yuntdağ Volcanics III. It is therefore, concluded that the mafic volcanic rocks probably correspond to the Yuntdağ Volcanics II. From the results of the absolute age determination, the mafic volcanic rocks indicate 14 to 15 Ma, hence it means that the mafic volcanism acted before or at the same time as the felsic volcanism.

The latest dacite-volcanism often forms lava domes in the Dikili-Bergama geothermal area. They NW-SE and ENE-WSW directions. The Yuntdağ Volcanics III can be subdivided trend in an ascending order into; biotite-hornblende andesite, dacite and rhyolite. Moreover, it is obvious that the volcanism in the latest stage formed the dome shaped Çam Tepe volcano which is composed of rhyolite lava 5 km east of Dikili. There is a possibility that the heat source for the present geothermal activity is derived from the post volcanic action of the Yuntdağ III volcanism. The absolute age, however, shows 14 to 16 Ma. That is, the data indicate that the Yuntdağ Volcanics III is older than the Demirtas pyroclastic rocks.

In the survey area, there are five hot springs at Nebiller, Kocaoba, Kaynarca, Dikili Ilıcasi and Pamuk Tepe. Three hot springs at Kocaoba, Kaynarca and Dekili Ilıcasi are discharging hot water above 60°C. Especially, Kaynarca hot spring discharges of boiling hot water.

Hydrothermal altered zones are distributed mainly in the Salihler-Gökceğül, Kocaoba, Sağancı-Ovacık, Kaynarca and Dikili Ilıcasi areas. Of these, the outcrops of mostly and wholly altered zones extend approximately 18.5 km<sup>2</sup> in total. The altered zones were formed mainly in the areas of the Yuntdağ Volcanics I and the Some formations from Miocene time to Pliocene time. The rocks have undergone intensive hydrothermal alteration prior to the Yuntdağ II volcanism. Especially, the intense geothermal activity presumably formed a high temperature reservoir at depth at least from Kocaoba to Sagnıcı-Ovacık. It is inferred that the geothermal system in this area was controlled by the NW-SE trending fault. Moreover, quartz and calcite veins in Ovacık and Bayram Tepe are considered to have played the role of geothermal reservoir or a path for high temperature fluid.

In the survey area, alteration is divided into the following three stages; before sedimentation of the Soma formation, before the Yuntdağ II volcanism and after the Yuntdag III volcanism.

The hydrothermal alteration in the stage before Yuntdağ I volcanism acted chiefly from Kocaoba to Sağancı and around Dikili Ilıcasi. It is assumed that this alteration is closely related to geothermal activity resulting from the magmatism of the Yuntdağ Volcanics I during Miocene time. The acting fluid in this stage likely represents a neutral-acidic condition of pH and a temperature exceeding 150°C.

In the stage before the Yuntdağ II volcanism, the geothermal activity was vigorous in the Salihler-Gökceğül area. The activity derived from felsic volcanism and its acting fluid was of strongly acidic pH and a low temperature. The altered zone probably occurred as a result of the reaction with acidic fluid at shallow depths.

After the termination of the Yuntdag III volcanism, weakly altered zones of Type IV occurred around the Kaynarca hot spring. Accordingly the fact is very closely related to the present geothermal activity such as the Kocaoba, Kaynarca and Dikili Ilıcasi hot springs. The geothermal activity is caused by the Yuntdağ III volcanism. From the results of the absolute age determination, the Pliocene andesites represented larger values than 13 Ma.

#### II.2.4 Chemical characteristics and temperature of reservoir fluid

The chemical characteristics, temperature, etc. of the Dikili-Kaynarca system are

estimated from geochemical and hydrological survey as follows:

The Dikili-Kaynarca system is judged to be the most active geothermal system in survey area according to the results of chemical and isotopic analyses. The systems is considered to be made up of water-dominated fluid originating from meteoric water.

Except for neutral  $\text{HCO}_3$  type hot-water, the existence of Cl-rich water was assumed in this area but the origin of Cl ions could not be clarified at this stage.

Hot water in the Dikili-Kaynarca system is composed mainly of neutral  $\text{HCO}_3$  type water and the Cl-rich water seems to be mixed with the water. There is a possibility that hot water discharging from the Kaynarca area and the hot water discharging from the Dikili-Ilıcasi originated from the same reservoir at depth. The water in the system is thought to circulate not only in the volcanic rocks but also in the sedimentary rocks.

The meteoric water is though to recharge is the southern slope of the Kozak massif and migrate to the southwest. During migration, the water is heated by conduction of rocks related to magmatism. The circulation time from the recharge area to the discharge area (Kaynarca) are concluded to be more than 75 years. The circulation time seems to belong enough for the water to make up a hydrothermal system of considerable size, compared with other systems.

Considering high  $\text{PCO}_2$  and high  $\text{HCO}_3$  ion content in the reservoir, the neutral  $\text{HCO}_3$  ( $-\text{SO}_4$ ) type fluid of about  $200^\circ\text{C}$  must be reserved at a considerable depth.

Judging from isotope data, the  $\text{HCO}_3$  ( $-\text{SO}_4$ ) type fluid in this system seems to be reserved in large quantity. The reservoir temperature of the  $\text{HCO}_3$  ( $-\text{SO}_4$ ) type water discharging mainly from the Kaynarca hot-spring is estimated to be  $180$  to  $200^\circ\text{C}$  and from Dikili Ilıcasi is  $110$  to  $160^\circ\text{C}$ . There is a possibility of a  $220$  to  $230^\circ\text{C}$  reservoir at a deeper level.

To aid the understanding of the subsurface fluid behavior and reservoir structure, a geothermal model from a geochemical view-point has been made, Fig. II.2.8. Cl-rich water ( $\text{HCO}_3$ -Cl type water) and the sealing zone in this figures are presumed, but have not been proven.

The-fluid detected by Hg survey data (Figs. II.2.9 and II.2.10) are shown in Fig. II.2.3. The analytical results show that up-flow zones of geothermal fluid from deep level seem to be confined in and around Kaynarca and Dikili Ilıcasi. There are tectonic lines such as the NE-SW and NW-SE systems possibly related to geothermal activity.



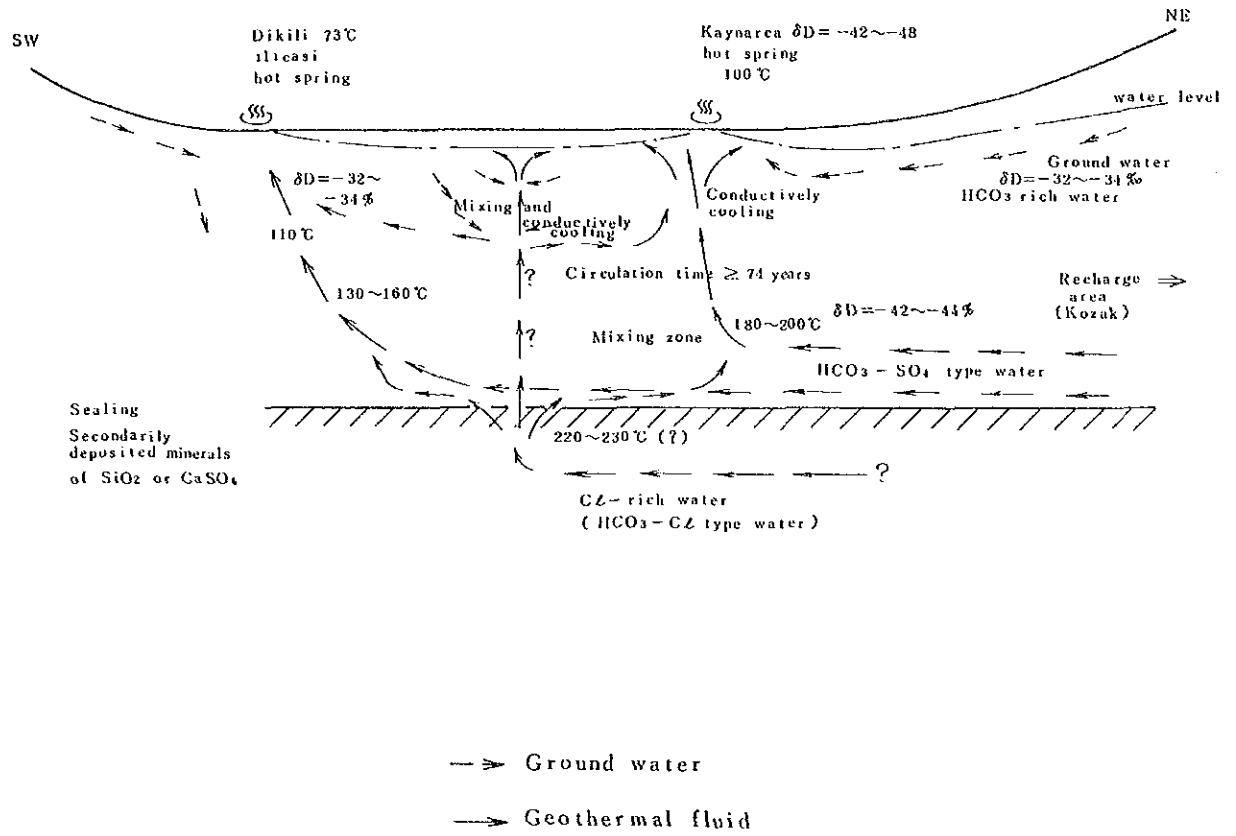


Fig. II.2.8 Hydrogeochemical model of the Dikili-Kaynarca system in the Dikili-Bergama geothermal field



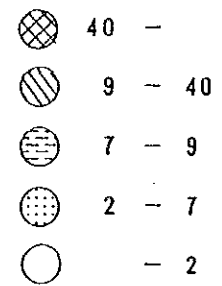
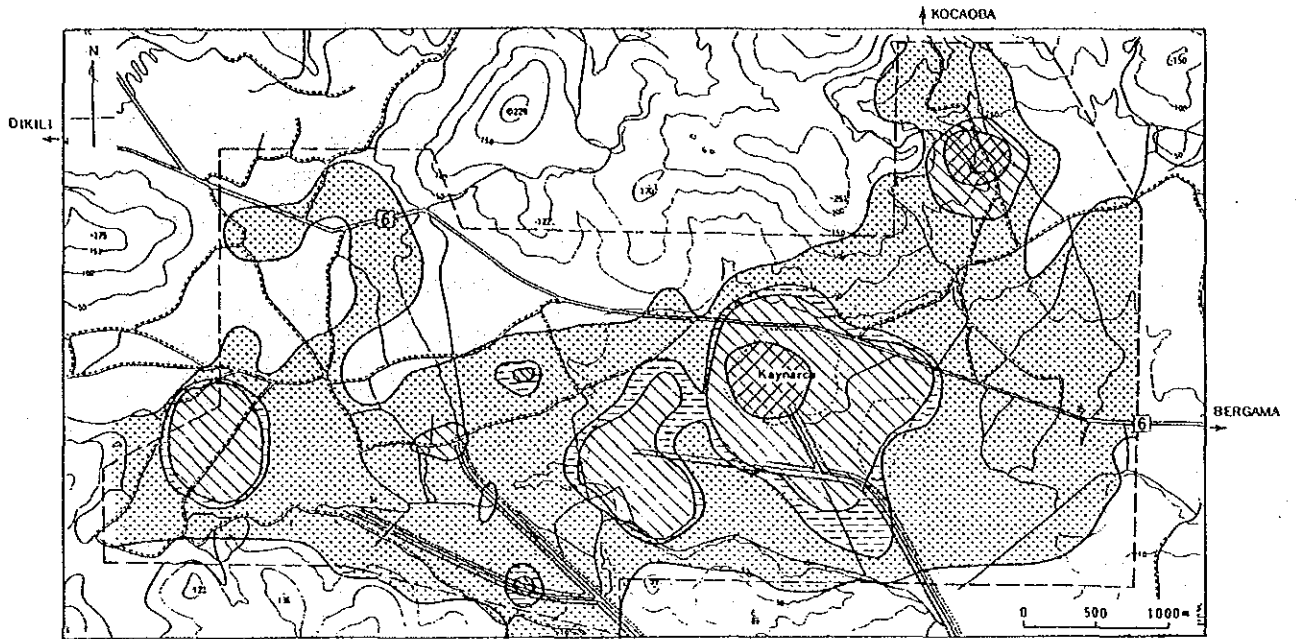


Fig. II 2.9 Smoothed iso-concentration contour map of Hg in soil gas

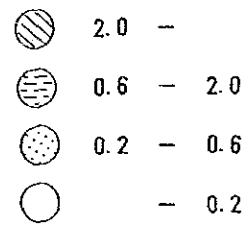
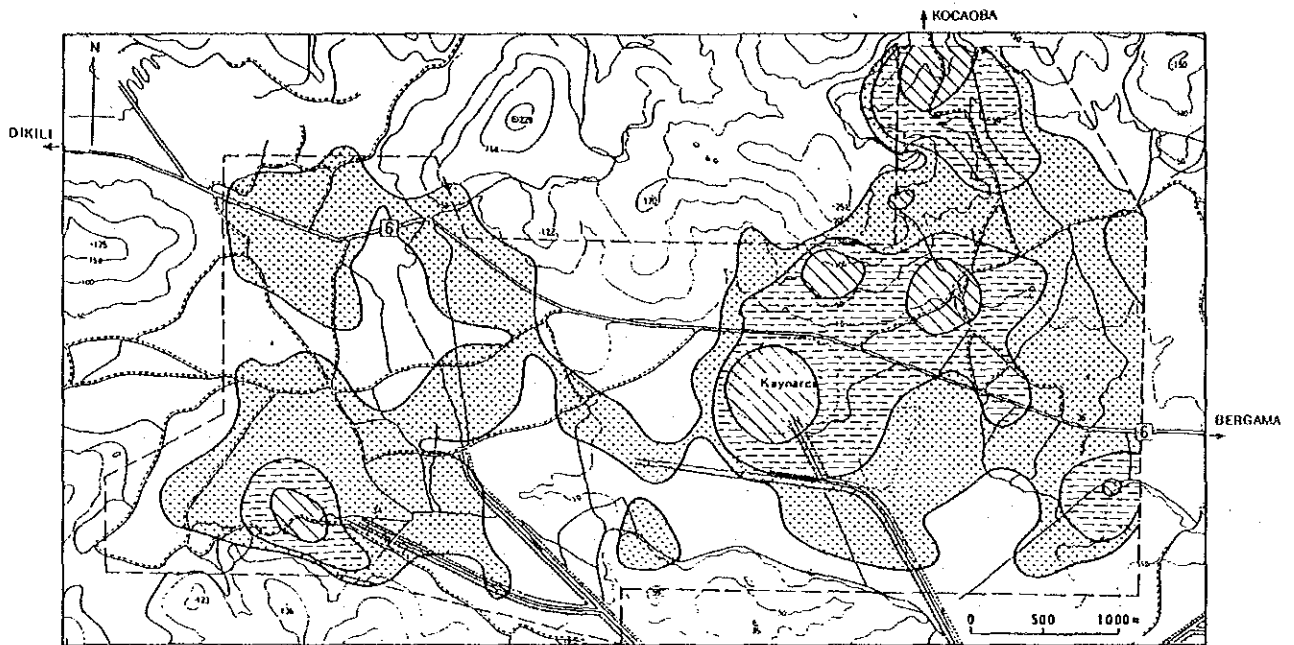


Fig. II 2.10 Smoothed iso-concentration contour map of Hg in soil



It is possible to consider that both the lines correspond to the distribution of fracture zones along faults.

In view of geochemical characteristics of the Dikili-Kaynarca geothermal system, reservation of 180 to 200°C water of neutral to weakly alkaline HCO<sub>3</sub> type and relatively low content of salt can be expected in and around Kaynarca. Concerning the future development for electric power generation, however, problems such as a considerably deep reservoir, scale deposition in production wells (expensive steam supply system) and high noncondensable gas content (low efficiency of power generation) will probably be encountered.

### II.2.5 Conceptual model

Based on the results of the first stage and the second stage explorations, the conceptual geothermal model in and around the Kaynarca area which is situated in the western part of the Dikili-Bergama geothermal area was constructed.

The subsurface structure from Dikili Ilıcasi to Kocaoba through the Kaynarca hot-spring is considered to be characterized by NW-SE trending and WNW-ESE trending faults from the gravity and the geological data. The Dikili Ilıcasi hot-spring is situated on the NW-SE trending fault zone and the Kaynarca hot-spring is on the WNW-ESE trending fault zone. Moreover, the Kocaoba hot-spring probably exists at the intersection of NW-SE and NE-SW trending faults. Therefore, it is assumed that the above mentioned hot springs are coming up along fracture zones of faults. Especially, in the Kaynarca hot-spring, hot water discharges from a deep seated reservoir in the deep fractures.

Pre-Tertiary basement forms the NW-SE trending horst around the Dikili Ilıcasi hot spring, and a graben between Dikili Ilıcasi and Kaynarca. To the north of Kaynarca, the pre-Tertiary basement becomes shallower up to the Kocaoba hot spring. To the north from Kocaoba, the basement must depress, judging from the low gravity anomaly.

The heat source of the present geothermal activity is possibly derived from the post volcanic action of the Yuntdağ III volcanism and the latest magmatism in the subsurface. This has not been proved yet.

The reservoir is expected to be not only in a shallow part of alluvial deposits but also in lava flows of Yuntdağ Volcanics I. Tuff breccias in the Yuntdağ Volcanics I and the Soma Formation possibly act as cap rock for the deep reservoir.

It is considered that the geothermal fluid at depth migrates horizontally on the top of pre-Tertiary basement, and circulates vertically along the faults.

## II.2.6 Selection of the prospective area for the third stage exploration

From the results of the second stage exploration, the area (42 km<sup>2</sup>) in and around Kaynarca (named “the Kaynarca geothermal area” in this report) was selected as the most prospective area compared with other areas in the Dikili-Bergama geothermal area. The third stage exploration was undertaken in this area for evaluation of geothermal potential.

## II.3 Results of the third stage exploration

### II.3.1 Detailed geological mapping

#### 1. Objectives

The detailed geological mapping was carried out in the most promising area selected from the results of the first and second stage explorations.

The objectives of the survey were to identify rocks, formations and geological structures, and to complete a detailed geological map. Moreover, the relations between fractures and geological structures in the survey area were investigated by the analysis of fracture patterns. Finally, the relations between these geological events and geothermal activities were discussed.

#### 2. Results of the investigation

##### (1) Topography

The survey area centered around Kaynarca is 6 km from north to south, 7 km from east to west and covers about 42 km<sup>2</sup>.

The area can be divided into three regions based on topographic features; a mountainous area to the north of Kaynarca, a lowland extending east and west through Kaynarca and a mountainous area to the south of Kaynarca.

The northern mountains are formed by Boz Tepe (331 m), Koca Tepe (319 m), Dede Tepe (251 m), Çam Tepe (229 m) and Kale Tepe (177 m). Most of the mountain slope is gentle, whereas the northwest slope of Çam Tepe and the southeast slope of Dede Tepe are steep and are linear.

A northeast trending valley lies between Kale Tepe and Çam Tepe and a northwest trending valley between Koca Tepe and Boz Tepe. The

Geyikli river which originates in the southwest foot of Kozak mountain flows along the valley between Kale Tepe and Çam Tepe. A large quantity of water flows along the valley during the rainy season and even during the dry season much water flows as subsurface flow. The valley from Kiroba to the northwest foot of Çam Tepe in which the Geyikli river flows is straight. It suggests the existence of a fault.

The northeastern part of the survey area where comparatively old volcanic crop out has a gentle dissected topography. Distinct fault scarps are found at some places along the east-west trending valley 500 m to the north of Dede Tepe.

On the other hand, in the southwestern part of the survey area, lava domes form Kargın Tepe (89 m), Maşat Tepe (74 m), Evrenşem Tepe (333 m).

In the central and southeastern part of the survey area, there is lowland below 10 m in altitude. The areas below 5 m form swamps. The lowland is a long and narrow basin, 5 km from east to west and 2 km from north to south around Kaynarca. The area is connected to neighboring lowland to the northwest and southeast of the area. The swampy areas found around Kaynarca are situated surrounding hot springs and trend in a northwest to southeast direction.

## (2) Geology

### 1) Stratigraphy

The geology of the area is composed of the Yuntdağ volcanics I (T<sub>yu1</sub>), Demirtaş pyroclastic rocks (Tp), Yuntdağ volcanics II (T<sub>yu2</sub>), III (T<sub>yu3</sub>) and Alluvium. This is shown in Table II.3.1, Geologic succession. Fig. II.3.1 shows the Bird's-eye view of the Kaynarca geothermal area, Fig. II.3.2 shows the Geological map and Fig. II.3.3 shows the Geological cross sections. Pre-Tertiary basement rocks (Mp), Kozak pluton (Tk) and Soma formation (Ts) are presumably distributed in the subsurface.

In this survey, the Yuntdağ volcanics III could be subdivided into six lavas; Koca Agıl hornblende andesite (Koca Agıl lave), Dikili biotite-hornblende andesite (Dikili lava) Çam Tepe dacite, Çam Tepe rhyolite, Koca Tepe biotite-hornblende andesite (Koca

Table II 3.1 Geological succession of the Kaynarca geothermal area

Age	Geologic column		Rock name	Geothermal activity	
Holocene		Alluvium			
Neogene	Pliocene	Yuntdağ volcanics III (Tyu3)	Sulu Kaya biotite-hornblende andesite	Hornblende - biotite andesite	?
			Koca Tepe biotite-hornblende andesite	Hornblende - biotite andesite	
			Çam Tepe rhyolite	Rhyolite	
			Çam Tepe dacite	Biotite dacite	
			Dikili biotite-hornblende andesite	Hornblende -biotite andesite	
			Koca Ağıl hornblende andesite	Hornblende andesite, Pyroxene -hornblende andesite	
	Miocene	İslamlar Pyroxene andesite (Yuntdağ volcanics II) (Tyu 2)	Basalt, Pyroxene andesite, Hornblende - pyroxene andesite		
		Demirtas pyroclastic rocks (Tp)	Felsic pyroclastic rocks, dacite, ignimbrite		
	Soğancı hornblende andesite (Yuntdağ volcanics I) (Tyu 1)	Hornblende andesite biotite - hornblende andesite, altered andesite			

Yuntdağ volcanism I

Felsic volcanism

Yuntdağ volcanism III

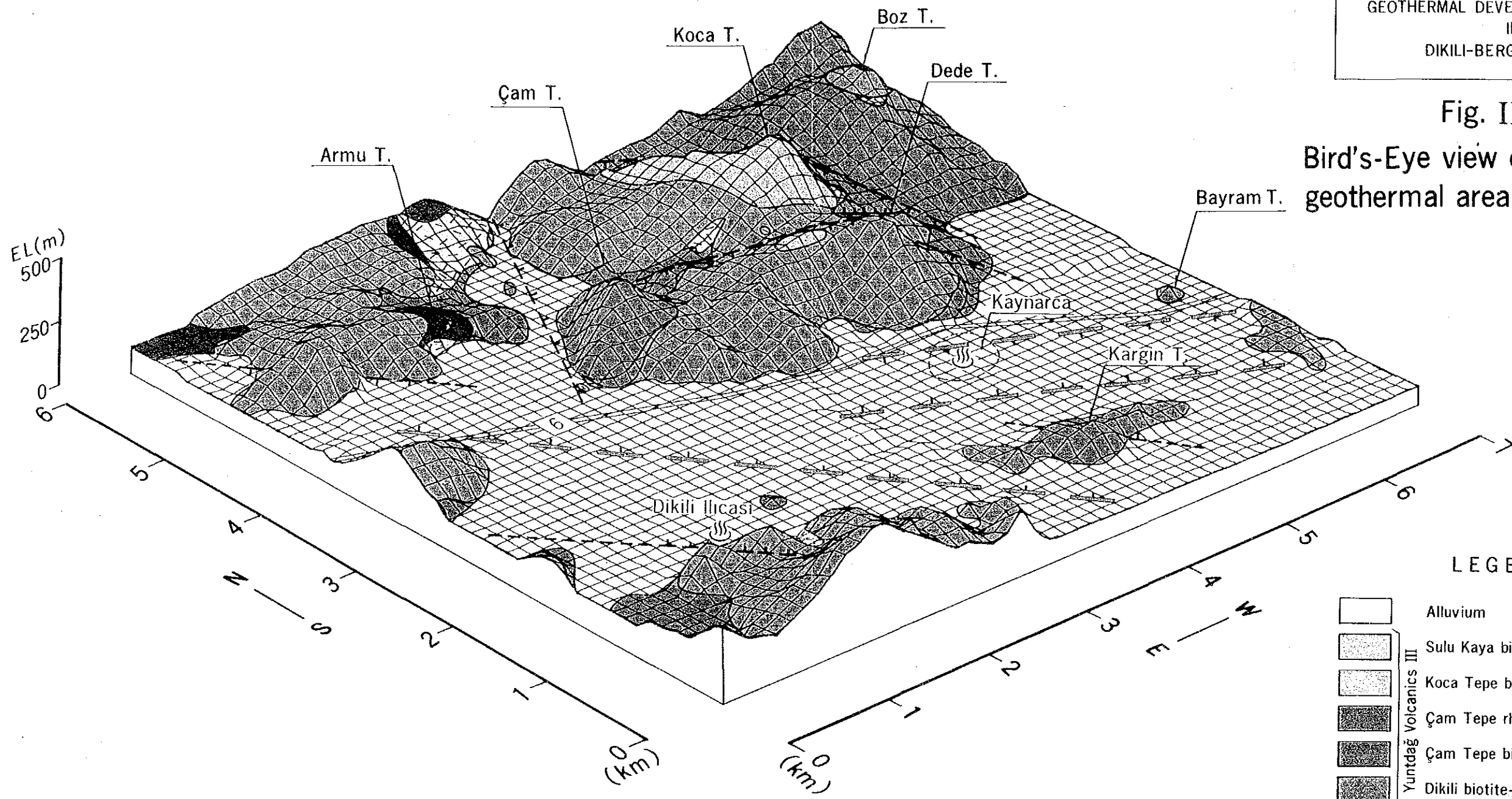
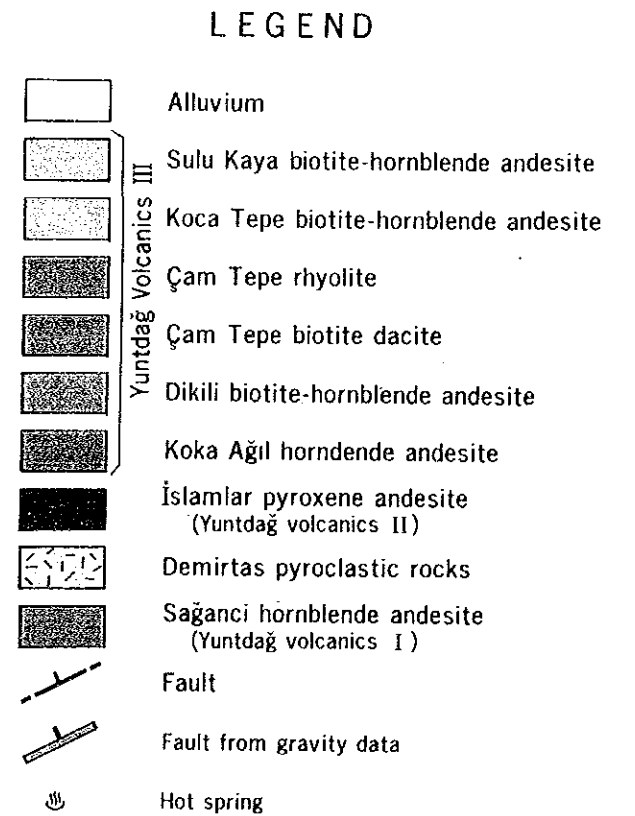


Fig. II.3.1  
Bird's-Eye view of the Kaynarca geothermal area



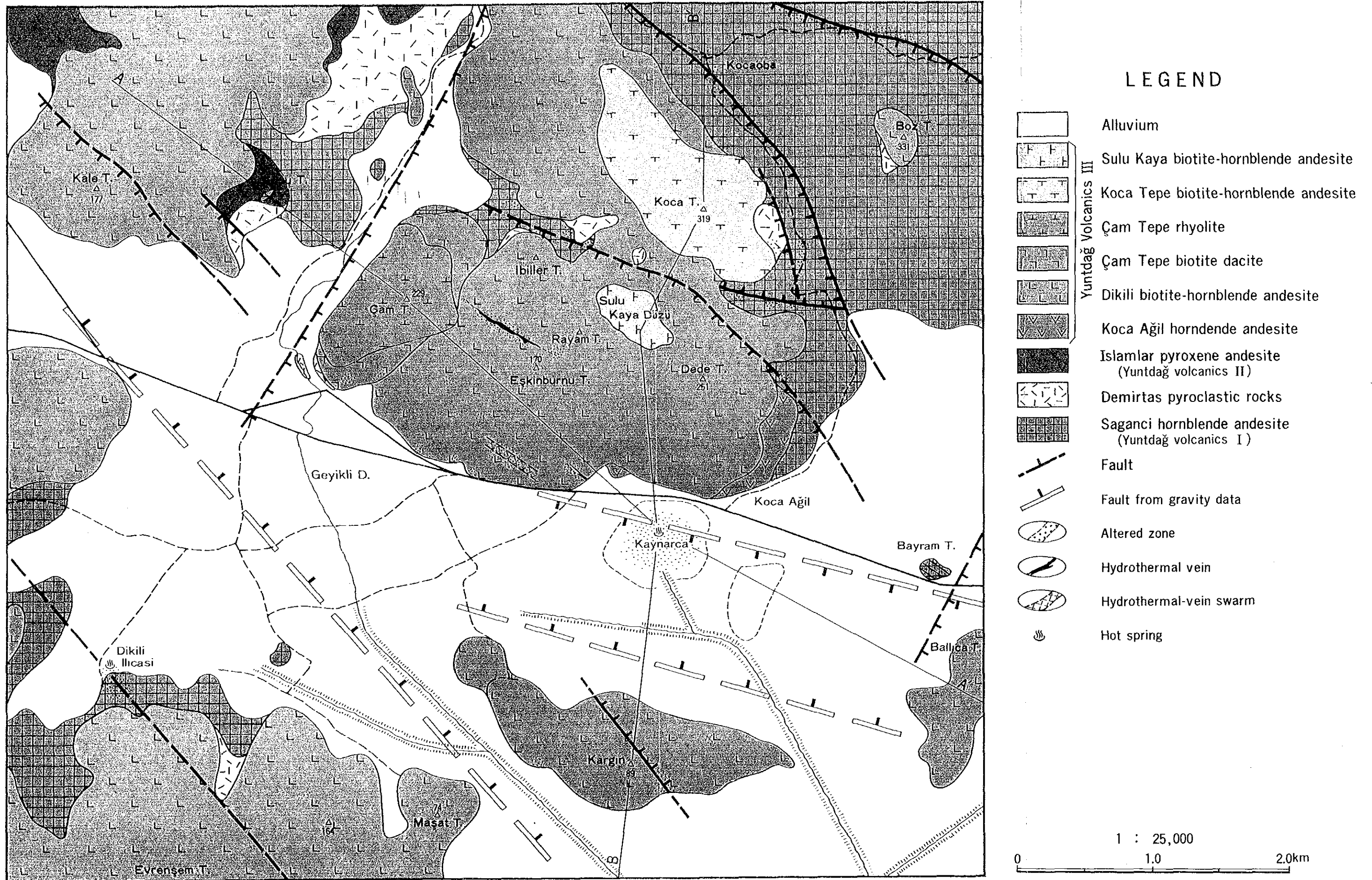


Fig. II .3.2 Geological map of the Kaynarca geothermal area

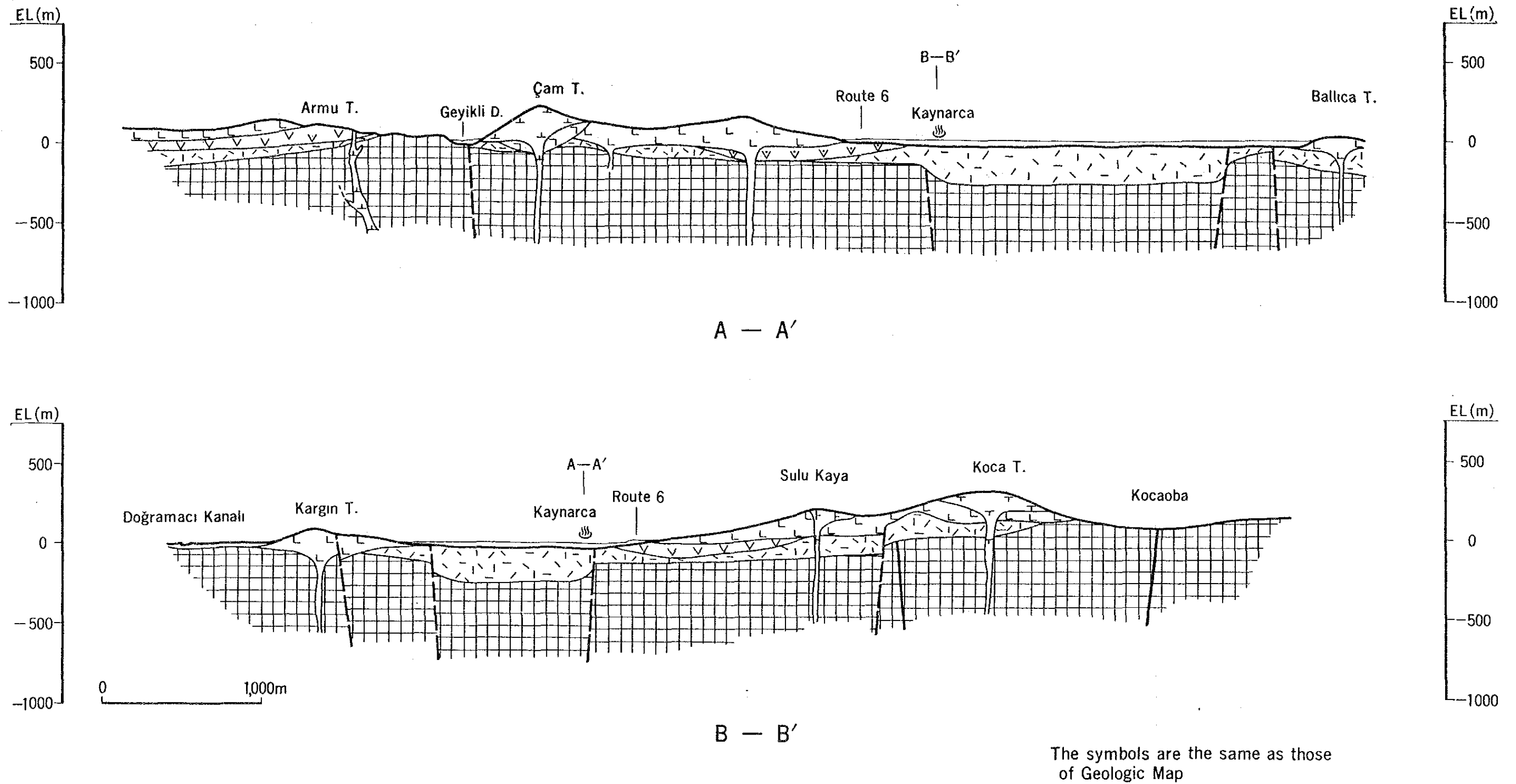


Fig. II.3.3 Geological cross sections of the Kaynarca geothermal area





Tepe lava), Sulu Kaya biotite-hornblende andesite (Sulu Kaya lava).

The geological survey confirmed that the Koca Tepe lava and Sulu Kaya lava erupted during the latest period of the Yuntdag volcanics III that are distributed in the survey area.

2) Explanation of each formation

(a) Yuntdag volcanics I (T<sub>yu1</sub>)

The Yuntdag volcanics I are found in the northeast, northwest and southwest parts of the survey area. In the northern part, all volcanics belong to the Yuntdag volcanics I except the top of Boz Tepe.

Most of the rocks are directly and horizontally covered by the Demirtas pyroclastic rocks, however, they are overlain by the Demirtas pyroclastic rocks on the east slope of Koca Tepe and around Armu Tepe.

The rocks consist mainly of hornblende andesite lava and occasionally intercalates with cognate tuff breccia. The rocks have mostly undergone hydrothermal alteration and have changed to light gray or dark-greenish gray altered rock. Some cracks in the rock are filled with silica mineral, calcite and gypsum. Moreover, silicified alteration zones and clayey zones are often found in the rocks.

The Yungtag volcanics I overlie the pre-Tertiary rocks widely and the maximum thickness is estimated to reach 1,500 m. It can be thought that the area where the rocks outcrop is upheaval part from the point of geotectonics.

Some east-west fault scarps in the rocks are found in the valley about 500 m to the north of Dede Tepe. Along the scarps silicified zones are exposed. There are many vertical slickensides on the fault plane in places.

At Bayram Tepe 2 km to the east of Kaynarca, many veins occur in the hydrothermal alteration zone of the Yuntdag volcanics I as if they are sinter. The veins are filled with idiomorphic crystals

of calcite and quartz. The veins generally strike N39° to 70°W and dip 70° to 90°NE and maximum width of veins reaches 20 m. In the meantime, Ballica Tepe which is situated about 500 m to the south of Bayram Tepe is made up of unaltered Yuntdağ volcanics III. It appears that the geological features of both sites are quite different. Accordingly the existence of a fault is presumed between Bayram Tepe and Ballica Tepe.

(b) Demirtas pyroclastic rocks (Tp)

The demirtas pyroclastic rocks are widely distributed in and around Demirtas about 10 km to the southeast of the survey area. In the survey area, the rocks are isolated on the right side of Geyikli river, in the river bed at the southwest foot of Çam Tepe, southwest foot of Koca Tepe, east foot of Koca Tepe, around Boz Tepe peak and southeast area of Dikili Ilıcasi, respectively.

The rocks directly overlie Yuntdağ volcanics I and their elevations vary at each outcrop from several meters to one hundred and scores of meters. For example, the rocks are found at an elevation of about 300 m around Boz Tepe peak, and are found at 10 to 20 m elevation at the southwest foot of Çam Tepe. The difference is about 300 m. This fact suggests the movement of a fault in the area after eruption of the Yuntdağ volcanics I.

The rocks are directly overlain with basalt or pyroxene andesite belonging to the Yuntdağ volcanics II in the northwest part of the survey area and in other areas.

The rocks consist mainly of felsic pyroclastic rocks, whereas on the right side of Geyikli river they are composed of dacite lava. In an outcrop at the southwest foot of Koca Tepe, pyroclastic rocks are light gray and contain many cognate rock fragments of 2 to 50 cm in diameter of hornblende andesite or dacite. There was no evidence to suggest that the rocks were deposited in water. They appear to have been deposited subaerially.

The thickness of the Demirtas pyroclastic rocks at the outcrops is less than 100 m, however, the rocks seem to have been deposited more thickly in the depression zone around Kaynarca.

A weak alteration zone is found only at the east foot of Koca Tepe and on the southeast of Dikili Ilıcasi.

The rocks are useful as a key bed to make clear the geologic succession and geological structure, because they are easily distinguished from the Yuntdağ volcanics I, and Yuntdag volcanics III and outcrops of the rocks are scattered all over the survey area.

(c) Yuntdağ volcanics II (Tyu<sub>2</sub>)

The Yuntdağ volcanics II are restricted to the northwestern part of the survey area.

The rocks overlie the Demirtas pyroclastic rocks and are covered by the Yuntdağ volcanics III.I.

The rocks consist of dark compact basalt and pyroxene andesite lava. They are the only effusive rocks of mafic volcanism in the survey area.

At the southeast foot of Armu Tepe, a rhyolitic dyke of 2 to 3 m width and trending northeast to southwest intrudes into the rocks. Moreover, a northwest trending fault is observed cutting the rocks and the Demirtas pyroclastic rocks to the southwest of Armu Tepe. In the rocks, a few small hydrothermal veins are found.

(d) Yuntdağ volcanics III (Tyu<sub>3</sub>)

The Yuntdağ volcanics III can be subdivided into six lavas based upon their petrographic and stratigraphic features. These lavas are the Koca Agıl hornblende andesite, Dikili biotite-hornblende andesite, Dikili biotite-hornblende andesite, Çam Tepe dacite, Çam Tepe rhyolite, Koca Tepe biotite-hornblende andesite, Sulu Kaya biotite-hornblende andesite.

(i) Koca Agıl hornblende andesite

Koca Agıl hornblende andesite is slenderly distributed along the south to south foot of Dede Tepe.

The Koca Agıl hornblende andesite is slenderly distributed along the south foot of Dede Tepe.

The lava consists of pyroxene-hornblende andesite and is the most mafic lava of the Yuntdağ volcanics III which are observed in the survey area. The lava is characterized by its dark gray color, compactness, few phenocrysts and rich platy joints. From these characters, this lava can be distinguished from the Dikili lava above.

The lava appears to exist in the subsurface of the Kaynarca geothermal area. There is a great possibility that shallow hot water is reservoired in the lava because it is obviously rich in fractures.

(ii) Dikili biotite-hornblende andesite

The Dikili biotite-hornblende andesite is found in most of the survey area and surrounding Kaynarca.

Most of the Yuntdağ volcanics III named in the 1st and 2nd survey are correlated with the lava. The lava is distributed mainly around Kale Tepe, Eşkinburnu Tepe, Pyam Tepe and Dede Tepe in the northern part of the survey area. In the southern part, the lava crops out around Evreşem Tepe, Maşat Tepe, Kargın Tepe and Ballica Tepe.

The lava directly overlies the Demirtas pyroclastic rocks around Koca Tepe, Dikili İlcasi and near the top of Boz Tepe. In other areas it overlies the Yuntdağ volcanics I, II and Koca Agıl lava. At the east foot of Çam Tepe and round Koca Tepe, Sulu Kaya Duzu, the lava is overlain by younger lava of the Yuntdağ volcanics III.

The lava generally consists of hornblende-biotite andesite. The lava which forms the northern mountain is characterized by its reddish dark gray color and compactness. On the contrary the lava of southern part of Kaynarca has a porphyritic texture. Phenocrysts of plagioclase, hornblende and biotite tend to be larger in size and greater in volume than that of the northern lava. Moreover, the former seems to be more mafic than the latter.

As a whole, the topography formed by the lava is a mixture of lava domes and lava flows. From the topography and flow texture in the lava, the direction of the lava flow appears to be west or

southwest trending around Dede Tepe and Payam Tepe, and to be northwest trending around Koca Tepe.

Weak or intermediate alteration is often found along hydrothermal veins. For example, many veins and alteration zones exist along the valley to the southwest of Payam Tepe, south foot of Eskinburnu Tepe and southwest foot of Koca Tepe. In the lava, not only quartz veins or calcite veins extend along a fixed direction but also network veins are observed. The existence of these veins show that the geothermal activity took place after the Dikili lava erupted.

(iii) Çam Tepe Dacite

The Çam Tepe Dacite is found at the foot of Çam Tepe and the area of the lava extends northeast to southwest.

The lava is overlain by the Çam Tepe rhyolite and directly covers the Dikili biotite-hornblende andesite.

The lava consists of dacite which is abundant in coarse-grained phenocrysts of biotite and plagioclase. In some parts of the south foot of Çam Tepe, the lava has undergone weak hydrothermal alteration, and small silica veins are found at the south foot of Çam Tepe.

(iv) Çam Tepe Rhyolite

The Çam Tepe rhyolite forms the peak on the northwest slope of Çam Tepe.

In this survey, it was discovered that the lava overlies the Çam Tepe dacite, and Dikili biotite-hornblende andesite. Therefore the lava is formed by one of the latest periods of volcanism in the survey area.

The lava consists of light gray, compact rhyolite and contains a few fine-grain phenocrysts of quartz and biotite. It shows remarkable flow texture and platy joints.

The western side of Çam Tepe forms a linear topographic feature

extending from northeast to southwest, which suggests the existence of a fault. At Armu Tepe to the northwest of Çam Tepe, a similar rhyolite intruded into the basalt lava of the Yuntdağ volcanics II. This rhyolite may belong to the Çam Tepe rhyolite.

(v) Koca Tepe biotite-hornblende andesite

The Koca Tepe biotite-hornblende andesite flowed down to the northwest and southeast from the peak of Koca Tepe.

The lava mostly overlies the Dikili lava, but in the southeast part, it directly overlies the Demirtas pyroclastic rocks.

The lava consists of biotite-hornblende andesite which is similar to the Dikili lava, but the volume of phenocrysts in the lava is larger than in the Dikili lava.

The lava appears to result from the youngest period of volcanism in the survey area.

(vi) Sulu Kaya biotite-hornblende andesite

The Sulu Kaya biotite-hornblende andesite flowed down only to the northwest from Sulu Kaya duzu where there is a col between Dede Tepe and Payam Tepe.

The lava directly overlies the Dikili lava, so that it was probably derived from the latest period of volcanism, being similar to the Koca Tepe lava in the survey area.

3) History of volcanism

Volcanic activity observed in the survey area is as follows:

- a) Yuntdağ volcanism I of middle Miocene age
- b) Demirtas felsic volcanism of middle Miocene age
- c) Yuntdağ volcanism II of middle Miocene age
- d) Yuntdağ volcanism III from middle Miocene time to Pliocene time

The Yuntdağ volcanism I occurred in the southwestern slope of

the Kozak massiff. The volcanic activity erupted a large volume of hornblende andesite to form a wide and flat lava plateau. The thickness of the plateau lava is estimated to be a maximum of about 1,500 m.

After that, a period of large tectonic activity took place in the area. The northern part of the plateau in the survey area was affected by uplift, whereas the area from the center to southwest part is affected by subsidence leading to the formation of the graben around Kaynarca as a center.

The following Demirtas felsic volcanism took place. Felsic pyroclastic rocks accumulated during the later stage of sedimentation of the Soma Formation. The activity center of the volcanism is probably situated around Demirtas, in the southwestern part of the survey area. The pyroclastic rocks are scattered on a small scale all over the survey area.

Yuntdağ volcanism II occurred in the same field of the felsic magmatism. The volcanic activity became a little mafic. As a result, basalt and pyroxene andesite lava flowed out. The lava is found in the northeast part of the survey area.

After that, many lava domes were formed by Yuntdağ volcanism III and gave rise to the original form of the present topography. The Yuntdağ volcanism III took place to the north of Kaynarca. This lava is composed of pyroxene-hornblende andesite. Afterwards, the Dikili lava flowed out all over the survey area. In some places, the lava is accompanied by agglomerate.

The following Çam Tepe decite might have erupted along northeast to southwest trending fissure vents. The Çam Tepe rhyolite was also erupted at the same place in the succession and formed a lava dome.

The center of the volcanism moved to the east, and finally the volcanic activity formed the lava domes such as Koca Tepe and Sulu Kaya Duzu. Therefore, this volcanism must be the latest one in the survey area. There is a possibility that the heat source for the present geothermal activity is derived from the post volcanic action of the younger Yuntdağ volcanism III.

(3) Geological structure

1) Faults and geological structure

In the survey area, there are three kinds of faults; NW-SE, NE-SW and WNW-ESE trending.

Fig. II.3.4 shows the main faults and the elevation at the upper boundary of the Demirtas pyroclastic rocks at each outcrop. The difference in elevation between each of the geological blocks shows the throw of the respective geological blocks.

(a) NW-SE fault running from east side of Koca Tepe to Kocaoba (F-1)

The fault cuts the Yuntdağ volcanics I and dips southwest. It is presumed that the throw is about 50 m judging from the difference in elevation of the Demirtas pyroclastic rocks.

Based on the result of the hydrothermal alteration survey, the rocks in the northeast area on the fault have undergone stronger alteration than those in the southwest area and are widely silicified.

(b) NW-SE fault from east side of Dede Tepe to the north side of Çam Tepe (F-2)

To the northwest of the fault, the Demirtas pyroclastic rocks crop out at 100 m to 200 m in altitude around Koca Tepe, whereas, these rocks to the southeast of the fault near Ibiller Tepe are found at 30 m to 50 m in altitude.

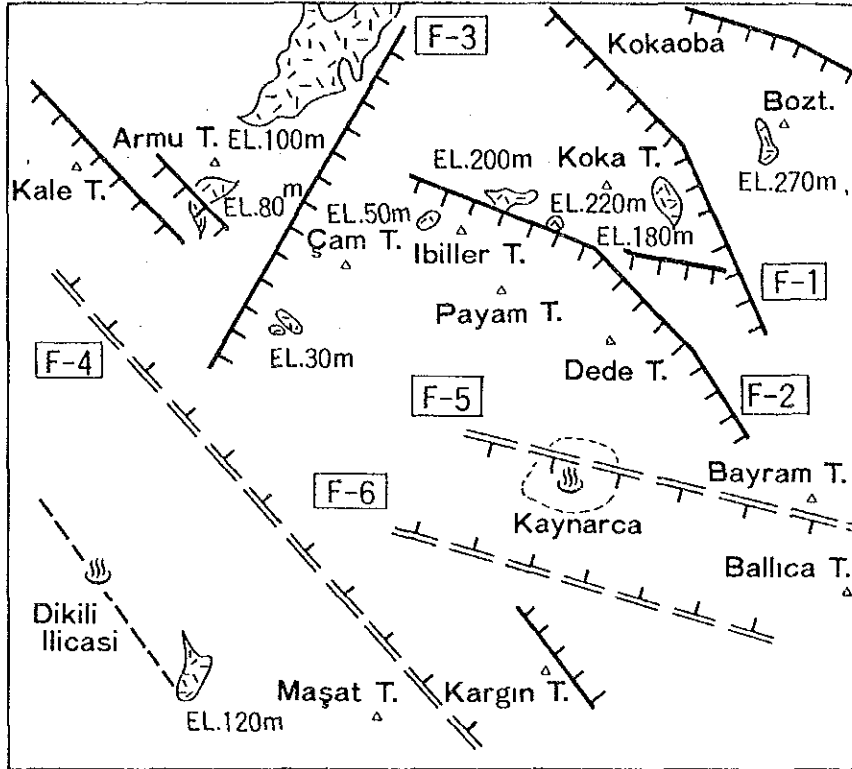
Moreover the Koca Agil hornblende andesite which is found to the south of the fault is not found to the northwest of the fault.

Therefore, it is assumed that the fault dips southwest and the throw is about 170 m.

(c) NE-SE fault through the west side of Çam Tepe (F-3)

The valley to the west of Çam Tepe linearly extend to NE-SW.





**LEGEND**

F-1~F-6 : Fault

EL. figure : Elevation of the upper boundary of the Demirtas pyroclastic rocks

Fig. II.3.4 Distribution of faults around kaynarca

The western side of Çam Tepe also forms a linear and steep slope. They suggest the existence of faults. In addition, from the results of the gravity survey a northeast trending fault seems to be situated on the west side of Çam Tepe.

The elevation of the Demirtas pyroclastic rocks in the northwestern area of the fault is higher than that of the southeast area of the fault. Consequently, the fault probably dips southeast.

- (d) NW-SE fault dipping NE in the northeastern side of Dikili Ilcasi (F-4), WNW-ESE fault dipping SE in the north side of Kaynarca (F-5) and WNW-ESE fault dipping NE in the south side of Kaynarca (F-6)

These faults are based on the gravity anomaly data and the distribution of Yuntdağ volcanics I. They appear to form the NW-SE trending depression zone to the west of Kaynarca and WNW-ESE trending depression zone to the east of Kaynarca.

The width of these zones is about 1 km and the depth of depression may be about 300 m.

The geological texture of the survey area is characterized by the NW-SE trending graben which is controlled by NW-SE trending step faults falling toward the central lowland. The graben trend changes to ENE-WSW east of Kaynarca.

The activity of the NW-SE trending faults began after the eruption of the Yuntdağ volcanics I and mostly terminated before the eruptions of the Yuntdağ volcanics III. Effusive materials from the Demirtas felsic volcanism and Yuntdağ volcanism III filled up the depression zone which was formed by the fault movement. Many NW-SE trending fractures and hydrothermal veins, however, are found in the Yuntdağ volcanics III. Therefore, it is assumed that the movement of the faults had continued after the time of the activity of the Yuntdağ volcanics III.

III.

Judging from the fact that the Dikili lava is cut by the NW-SE trending fault to the northwest of Çam Tepe and the younger Çam Tepe dacite and rhyolite flowed out as though along the

NE-SW trending fissures. As a result, the activity of the NE-SW faults possibly took place after the Dikili lava erupted.

## 2) Analysis of fracture patterns

In the geological survey, 558 fractures were measured from 137 outcrops. Fractures which are accompanied by hydrothermal veins and are continuous, were selected. The orientation (dip and strike) of a fracture was described by plotting the pole of the fractures on the projection plane using a Wulff-stereonet. The distribution the method of fractures, the method for contour diagram and presumption method of stress field are shown in Appendix A.1.

### (a) Fracture pattern

As shown in the following 4 figures, the results of the fracture measurement are divided by each formation and each part of the survey area.

- a. Fig. II.3.5  
Fracture pattern of the Yuntdağ volcanics I (Tyu<sub>1</sub>)
- b. Fig. II.3.6  
Fracture pattern of the Demirtaş pyroclastics rocks (Tp)
- c. Fig. II.3.7  
Fracture pattern of the Yuntdağ volcanics III (Tyu<sub>3</sub>)
- d. Fig. II.3.8  
Composite map showing the fracture pattern in the Kaynarca geothermal area

The characteristics of the fracture patterns in each area are as follows.

#### 1. Around Çam Tepe

In this area, fractures in the Demirtaş pyroclastic rocks and the Yuntdağ volcanics III were measured. The NE-SW and S-N trending fractures of the Yuntdağ volcanics III, the NE-

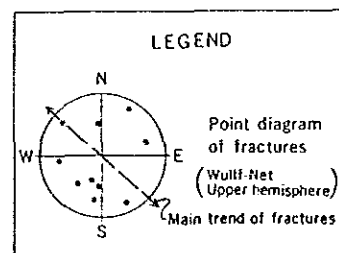
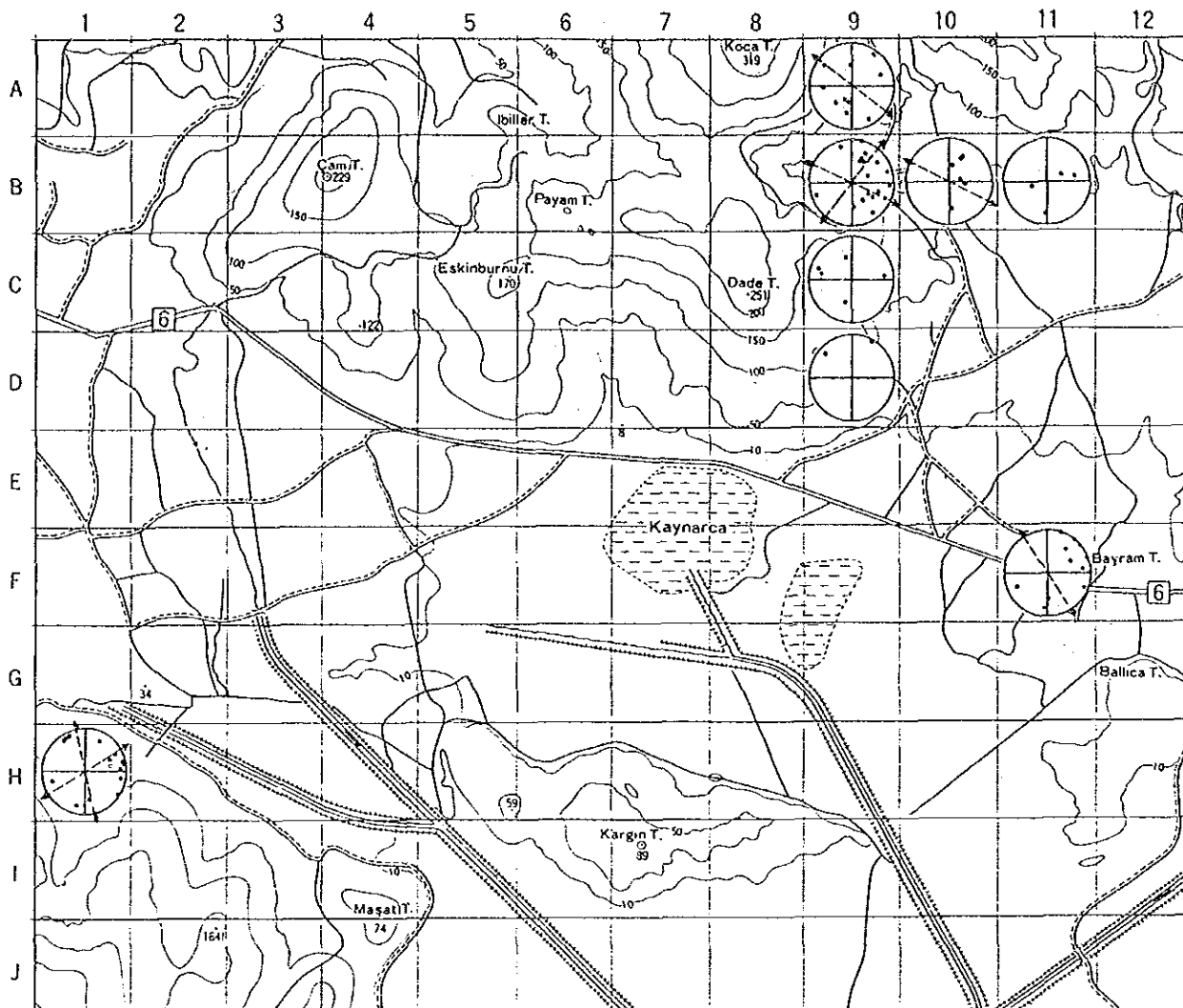


Fig. II.3.5 Fracture pattern of Yuntdağ Volcanics I in the Kaynarca geothermal area

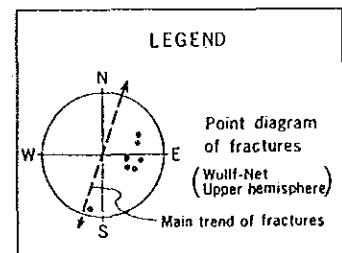


Fig. II .3.6 Fracture pattern of Demirtas pyroclastic rocks in the Kaynarca geothermal area

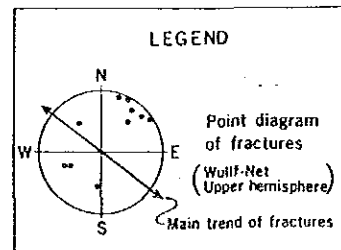
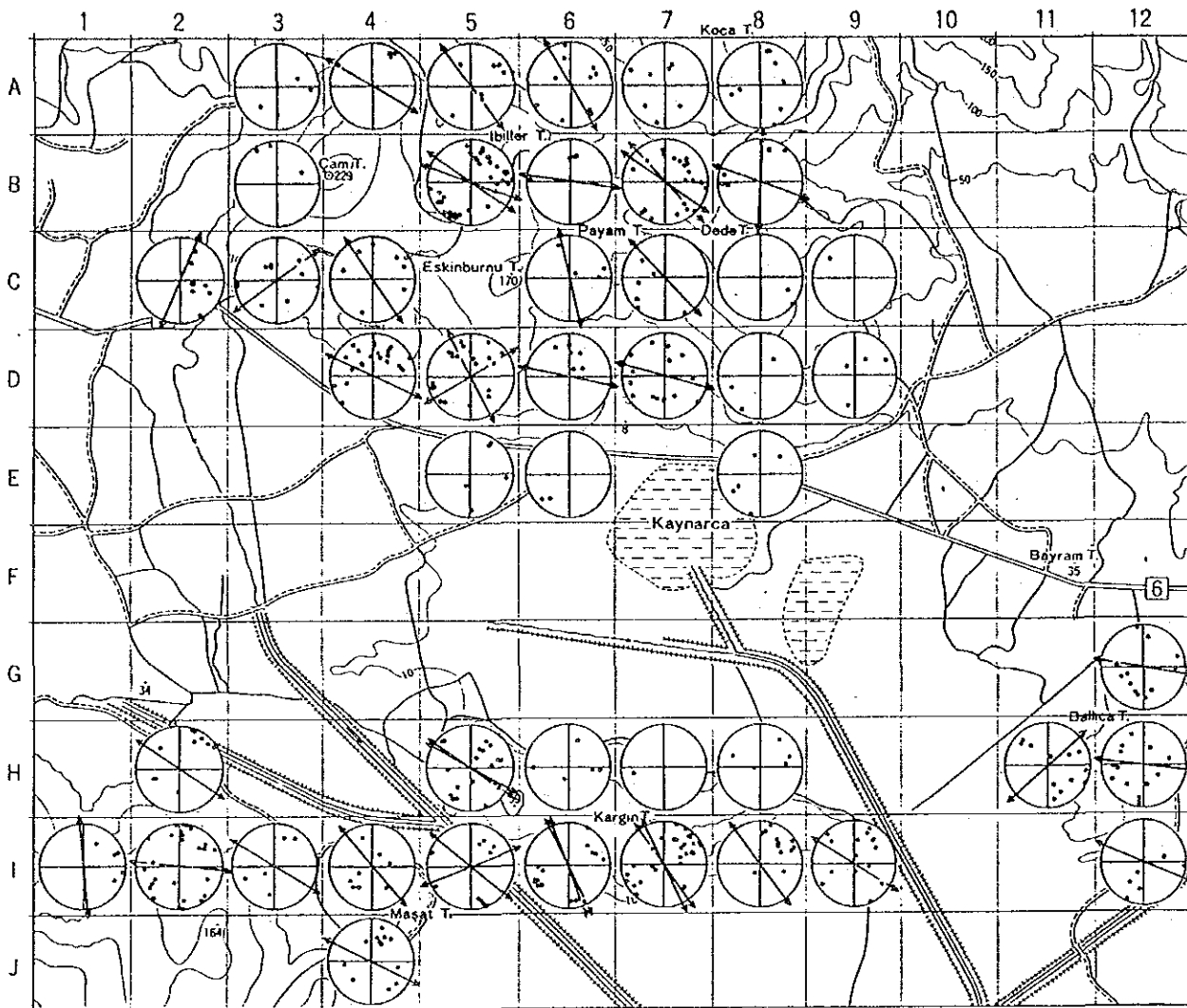


Fig. II.3.7 Fracture pattern of Yuntdağ Volcanics III in the Kaynarca geothermal area

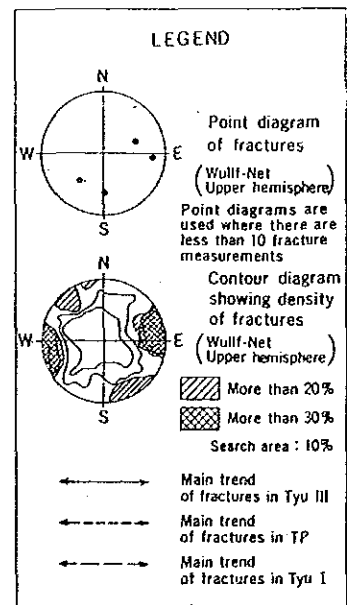
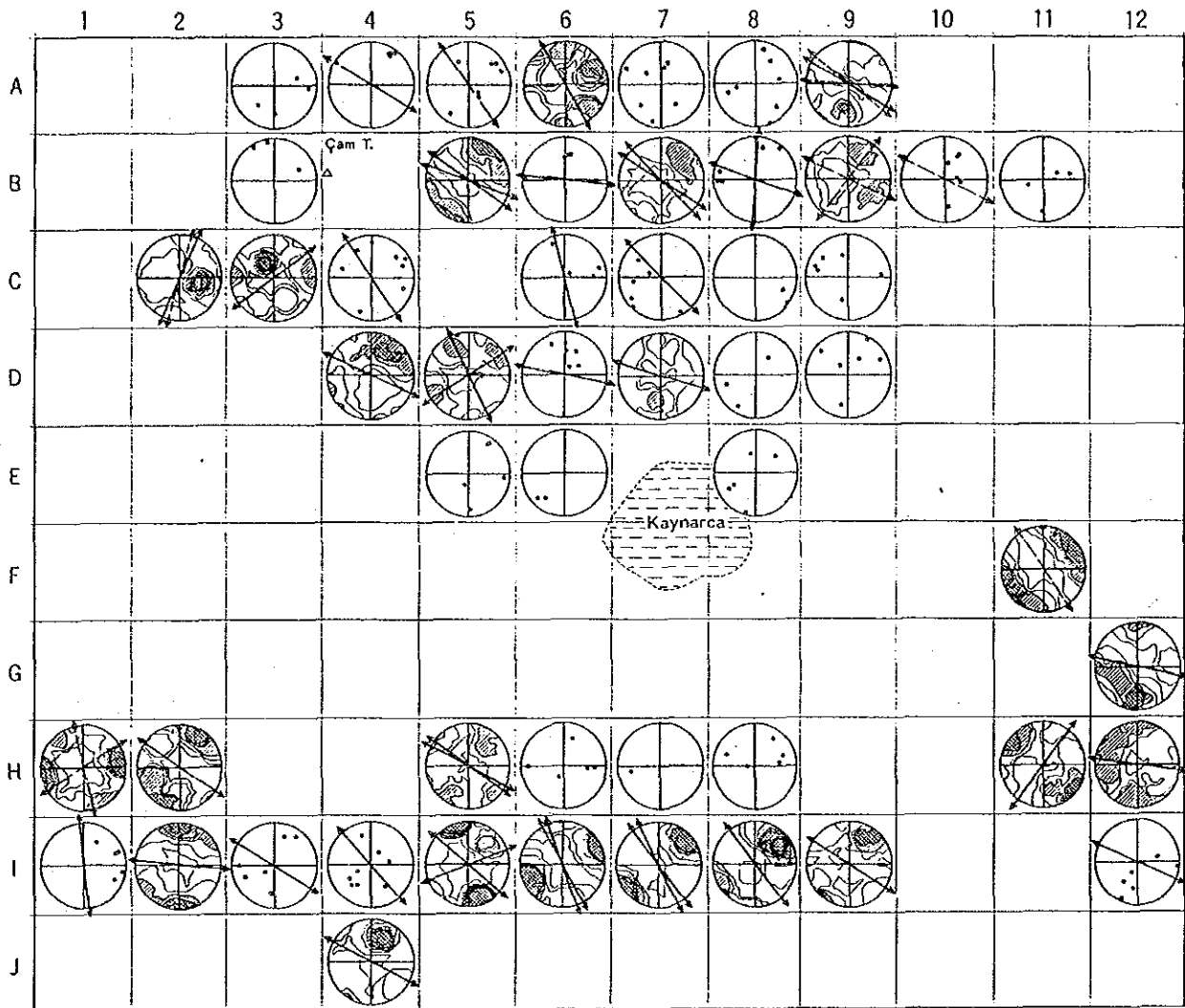


Fig. II.3.8 Composite map showing fracture pattern in the Kaynarca geothermal area